

Nonlinear Optics on Ferroics & Multiferroics

Introduction

Part I – Symmetry

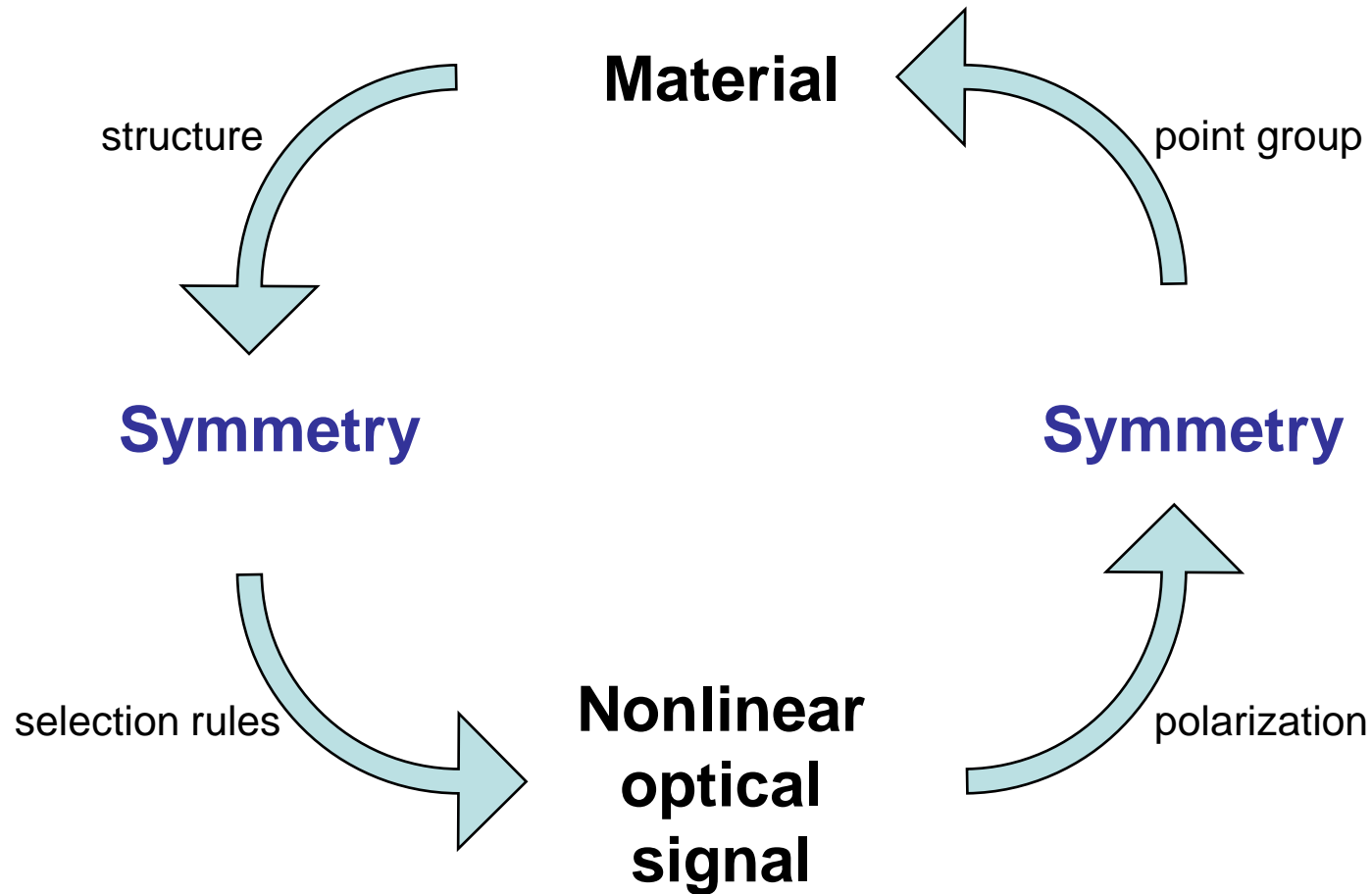
Part II – Nonlinear Optics

Part III – Experimental Techniques


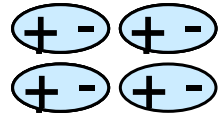
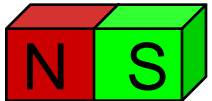
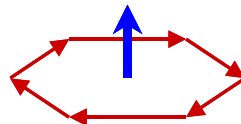
Part IV – Multiferroic $RMnO_3$

Thomas Lottermoser

Principle of Nonlinear Optical Structure Analysis



Symmetry and Multiferroics

Time \ Space	invariant	change
invariant	ferroelastic	ferroelectric
change	ferromagnetic	ferroquadrupolar
Time \ Space	invariant	change
invariant		
change		

**Ferroic properties
determine
space & time symmetry**

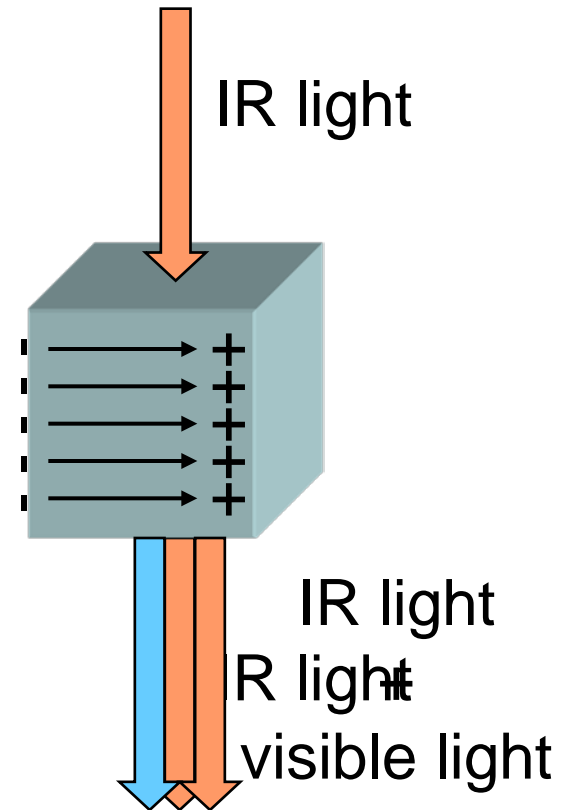
Symmetry and Nonlinear Optics

Case 1:

- Crystal in a paraelectric phase
- Inversion symmetry *not broken*

Case 2:

- Crystal in a ferroelectric phase
- Inversion symmetry *broken*

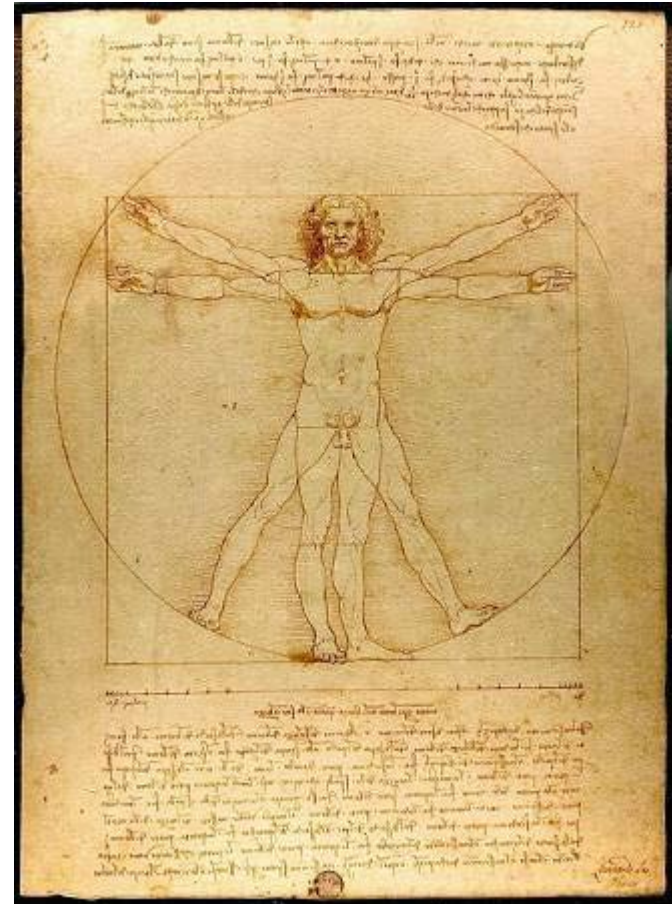


Literature

- General introductions to nonlinear Optics:
Y.R. Shen, A. Yariv, or R.W. Boyd
- K.H. Bennemann: Nonlinear Optics in Metals
- R.R. Birss: Symmetry and Magnetism

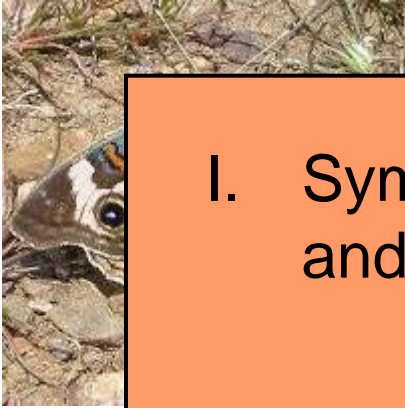
Part I - Symmetry

- Symmetry Operations
- Space & Time Inversion
- Tensors
- Point Groups



What's Symmetry?

Nature:



Art:



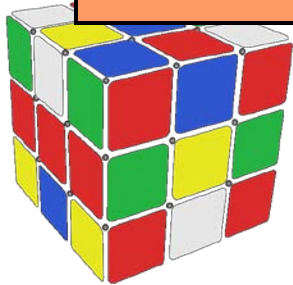
Architecture:



I. Symmetry is a property related to harmony and aesthetics

II. **Symmetry describes the behaviour under certain transformations**

Geo



What's Symmetry?

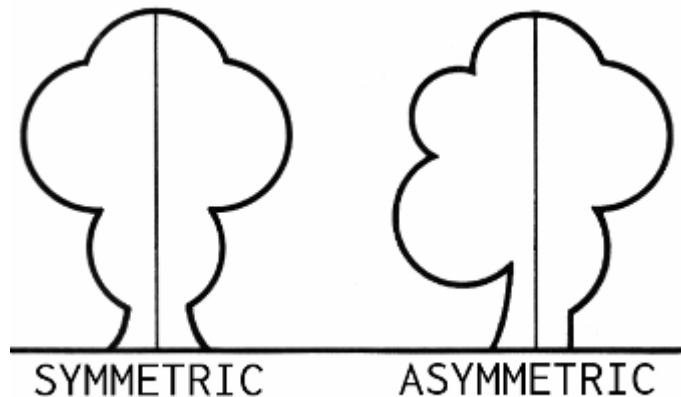
Symmetry:

Conservation of shape under applying a symmetry operation

Asymmetry:

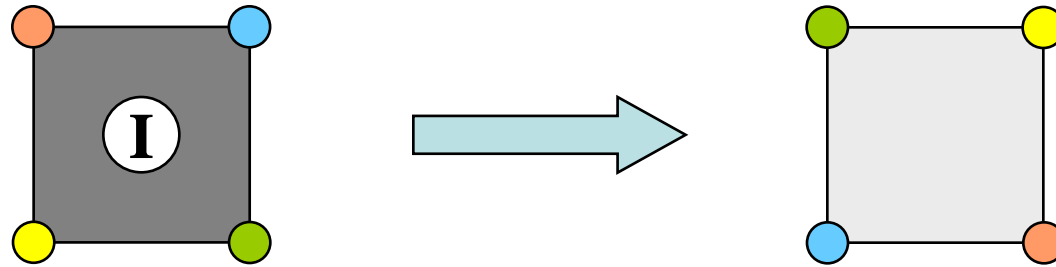
Change of shape under applying a symmetry operation

e.g. mirror symmetry

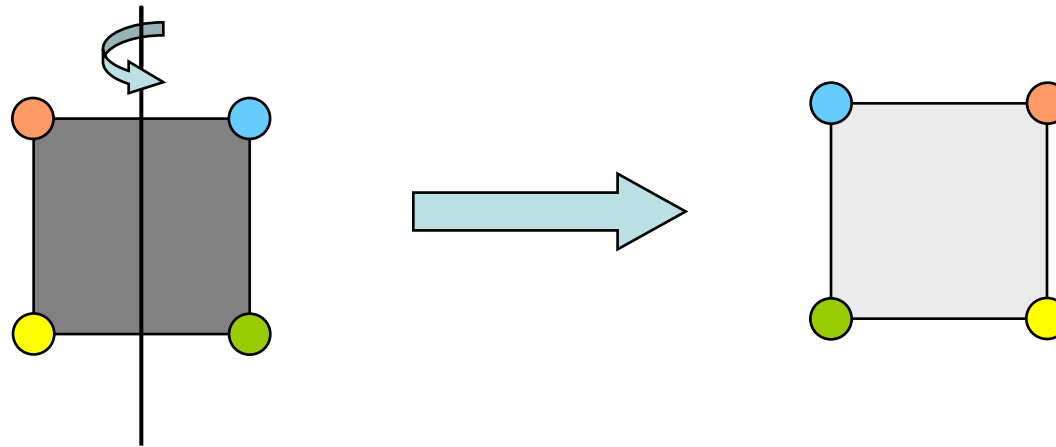


Symmetry Operations in Space

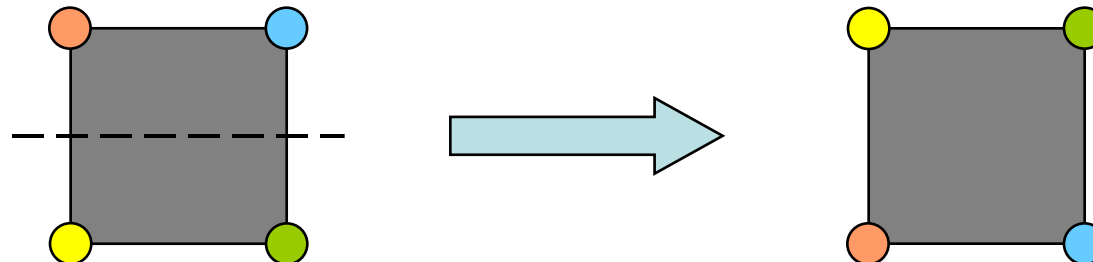
Inversion:



Rotation:

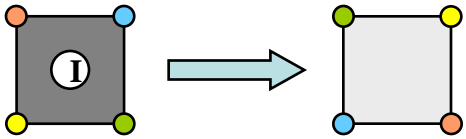


Mirroring:
(= I • R)



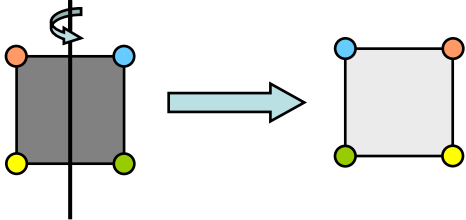
Mathematical Matrix Representation

Inversion:



$$I = \begin{bmatrix} -1 & 0 & 0 \\ 0 & -1 & 0 \\ 0 & 0 & -1 \end{bmatrix} \equiv [\bar{1}]$$

Rotation:

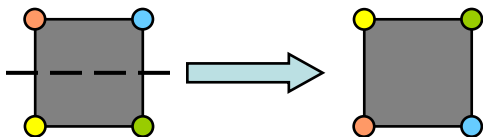


$$R(\varphi_y) = \begin{bmatrix} \cos(\varphi_y) & 0 & \sin(\varphi_y) \\ 0 & 1 & 0 \\ -\sin(\varphi_y) & 0 & \cos(\varphi_y) \end{bmatrix}$$

$$\Rightarrow R(180^\circ) = \begin{bmatrix} -1 & 0 & 0 \\ 0 & 1 & 0 \\ 0 & 0 & -1 \end{bmatrix} \equiv [2_y]$$

Mirroring:

(= I • R)

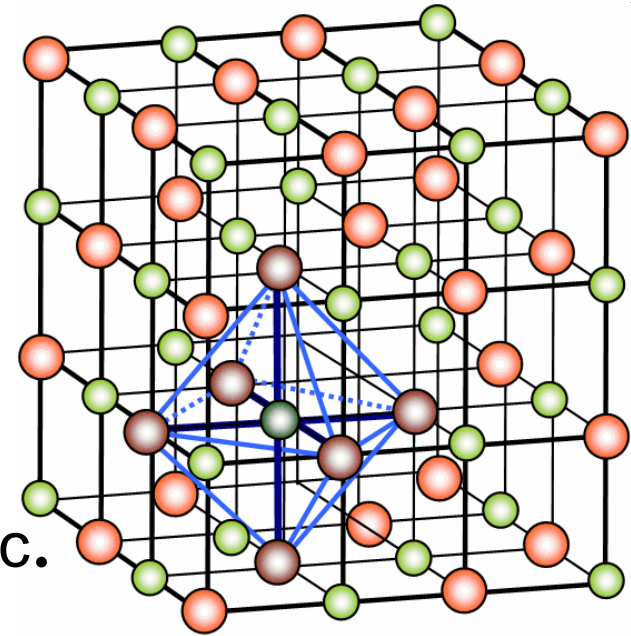


$$M_y = [\bar{1}] \cdot [2_y] = \begin{bmatrix} 1 & 0 & 0 \\ 0 & -1 & 0 \\ 0 & 0 & 1 \end{bmatrix} \equiv [\bar{2}_y]$$

Point Symmetries in Crystals

Only discrete symmetries in crystals:

- Identity operation: $[1]$
- Inversion: $[\bar{1}]$
- Rotations: $[1_x], [2_x], [3_x], [4_x], [6_x],$ etc.
- Mirror planes: $[\bar{2}_x], [\bar{2}_y], [\bar{2}_z],$ etc.



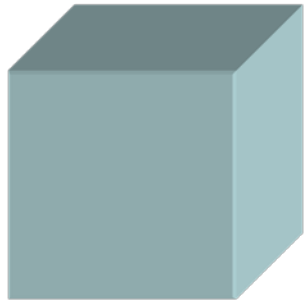
⇒ System of **32 point groups** with different subsets of symmetry operations

Symmetry and Physics

P. Curie, 1894: "C'est la dissymétrie qui crée le phénomène"


e.g.: Ferroelectricity:

I. Paraelectric phase:

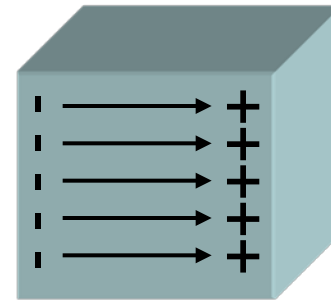


Cubic crystal with inversion symmetry

Phase
transition



II. Ferroelectric phase:



Polar tetragonal crystal without inversion symmetry

Curie's Principle

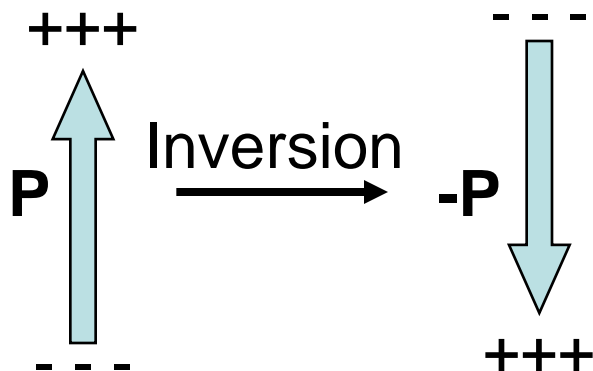
The symmetry of a crystal exhibiting a certain effect is the intersection of the symmetries of the bare crystal and the effect itself

$$\left. \begin{array}{l} \text{Crystal symmetry} = G_C \\ \text{Effect symmetry} = G_E \end{array} \right\} G_C \cap G_E \equiv G_{CE} \quad \text{Symmetry of crystal + effect}$$

Neumann's Principle

The physical properties of a crystal have at least the symmetry of the crystal

Example: Ferroelectricity



Electric polarization breaks inversion symmetry

⇒ *No* ferroelectricity in crystals possessing inversion symmetry!

Property & Field Tensors

Physical effects in crystals can be described by the equation:

$$\mathbf{E}_{\text{(effect)}} = \mathbf{P}_{\text{(roperty)}} \cdot \mathbf{C}_{\text{(ause)}}$$

\mathbf{E} , \mathbf{C} : Field tensors
 \mathbf{P} : Property tensor

} Anisotropic quantities
↳ Symmetry!

Examples:

- Dielectric displacement $\mathbf{D} \propto \boldsymbol{\varepsilon} \cdot \mathbf{E}$
- Magnetic induction $\mathbf{B} \propto \boldsymbol{\mu} \cdot \mathbf{H}$

Neumann's Principle & Property Tensors

Property tensors must be invariant under all symmetry operations of the crystal

Example: Second harmonic generation (SHG)

$$\mathbf{P}(2\omega) \propto \chi^{(2)} \mathbf{E}(\omega) \mathbf{E}(\omega)$$

$$\text{Inversion I} \Rightarrow -\mathbf{P}(2\omega) \propto \chi'^{(2)} (-\mathbf{E}(\omega))(-\mathbf{E}(\omega))$$

$$\Rightarrow \chi'^{(2)} = -\chi^{(2)} \quad \text{⚡ if inversion is symmetry operation}$$

\Rightarrow No SHG in crystals possessing inversion symmetry!

Classification of Tensors: Parity Operations

Symmetry operations with eigenvalues ± 1

Spatial inversion I

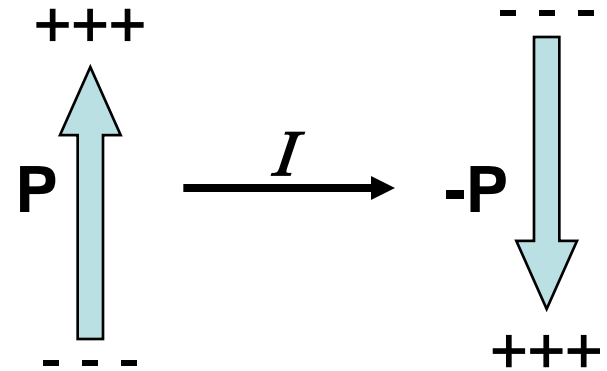
Time inversion T

Parity Operations: Spatial Inversion

Polar tensors:

$$I\vec{P}(\vec{r}, t) = -\vec{P}(-\vec{r}, t)$$

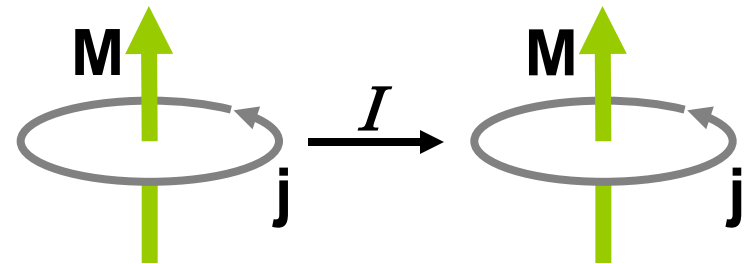
⇒ Polar tensors of *odd* rank are equal to zero in centrosymmetric crystals!



Axial tensors:

$$I\vec{M}(\vec{r}, t) = \vec{M}(-\vec{r}, t)$$

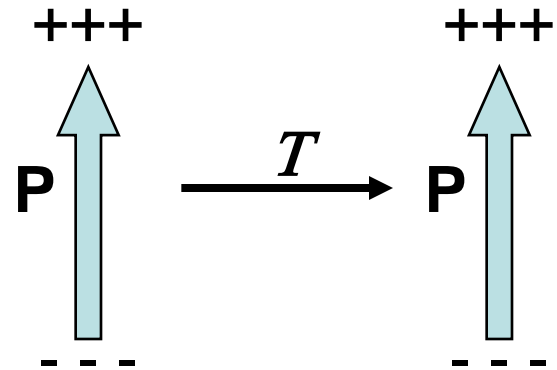
⇒ Axial tensors of *even* rank are equal to zero in centrosymmetric crystals!



Parity Operations: Time Inversion

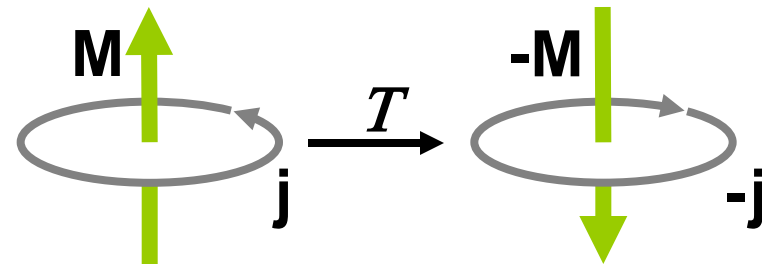
i-tensors:

$$T\vec{P}(\vec{r}, t) = \vec{P}(\vec{r}, -t)$$



c-tensors:

$$T\vec{M}(\vec{r}, t) = -\vec{M}(\vec{r}, -t)$$



⇒ c-tensors in non-magnetic crystals are equal to zero!

Time Inversion = Going Back in Time?

Answer: NO!

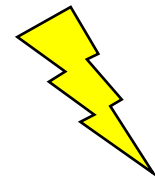
Here: Only static effects \leftrightarrow no increase of entropy!

e.g. electric current: $j_i = \sigma_{ij} E_j$

$\left. \begin{array}{l} j_i: \text{c-tensor} \\ E_i: \text{i-tensor} \end{array} \right\} \Rightarrow$ Neumann's principle:
 σ_{ij} must also be a c-tensor!



Only current flow in magnetic crystals!



In this context:

Time reversal equivalent to spin reversal!

General Classification of Symmetry Operations

1-, 2-, 3-, 4-, and 6-fold rotations \Rightarrow 11 Laue-groups

+ Spatial inversion I \Rightarrow 32 crystallographic point groups

+ Time inversion T \Rightarrow 122 magnetic point groups

+ Translation \Rightarrow 230 crystallographic space groups

Optical regime: $\lambda \gg a$

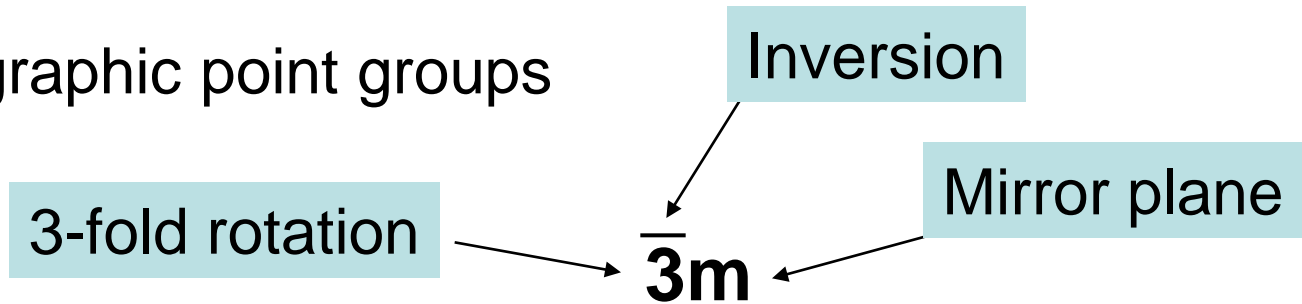
& 1651 magnetic space groups

Nomenclature of Point Groups

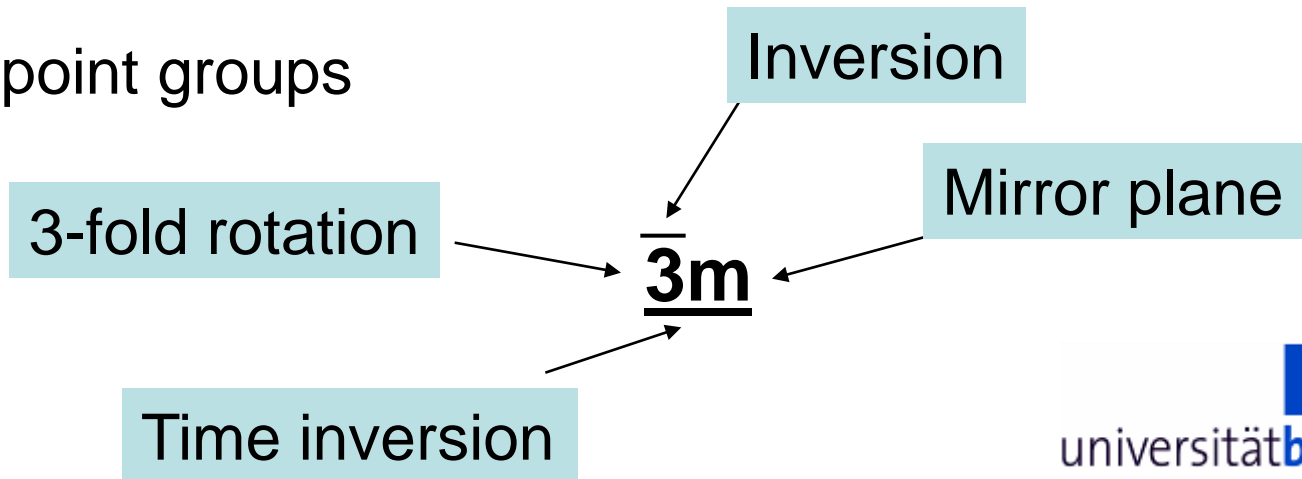
System after Hermann-Mauguin:

Directly derived from the allowed symmetry operations, but only 'significant' subset is used.

- I. Crystallographic point groups
e.g. $\bar{3}m$



- II. Magnetic point groups
e.g. $\underline{3}m$



'Forbidden' Effects

What symmetry *can not* do:

- No definite prediction of a certain effect
- No microscopic/quantitative description of physical effects

What symmetry *can* do:

- A prediction which effects are possible
- A prediction which effects are definitely forbidden

e.g. no ferroelectricity in centrosymmetric crystals

The Magnetoelectric (ME) Effect

$$P_i = \varepsilon_0 \chi_{ij}^e E_j + \frac{1}{c} \alpha_{ij} H_j \quad M_i = \chi_{ij}^m H_j + \frac{1}{\mu_0 c} \alpha_{ij} E_j$$

P_i, E_j = first rank polar i-tensors,
 M_i, H_j = first rank axial c-tensors

$\Rightarrow \alpha_{ij}$ = second rank axial c-tensor

Only allowed in
non-centrosymmetric crystals

Only allowed in
magnetic crystals

ME forbidden in at least 53 of
the 122 magnetic point groups!

How to Derive Tensor Components?

1. Be smart and solve for each allowed symmetry operation
 3^n equations of the type:

$$d_{ijk\dots n} = \sigma_{ip} \sigma_{jq} \sigma_{kr} \dots \sigma_{nu} d_{pqr\dots u}$$

2. Be even smarter and look them up in the book of Birss:

Symmetry and Magnetism

BY

ROBERT R. BIRSS

Senior Lecturer in Physics
University of Sussex, Brighton

Magnetoelectric Effect in Cr_2O_3

1. Symmetry and symmetry operations for Cr_2O_3

Tri- gonal	$\bar{3}m$	$\bar{6}\cdot m$	-	-	$1, \bar{1}, 3(2_{11}), 3(\bar{2}_{11}), \pm 3_2, \pm \bar{3}_2$	$\sigma^{(1)}, \sigma^{(2)}, \sigma^{(6)}$	-
	$\bar{3}m$	$\bar{6}\cdot m$	$\bar{3}$	$\bar{6}$	$1, \bar{1}, +3_2, +\bar{3}_2, 3(2_{11}), 3(\bar{2}_{11})$	$\sigma^{(1)}, \sigma^{(6)}$	$\sigma^{(2)}$
	$\bar{3}m$	$\bar{6}\cdot m$	32	3:2	$1, 3(2_{11}), \pm 3_2, \bar{1}, 3(\bar{2}_{11}), \pm \bar{3}_2$	$\sigma^{(2)}, \sigma^{(6)}$	$\sigma^{(1)}$

The magnetoelectric tensor in Cr_2O_3 :

2. The mag

System	Magnetic point group \mathcal{M}'
Fe_2O_3	$\bar{3}m$
Cr_2O_3	$\bar{3}m$
	$\bar{3}m$

$$\alpha = \begin{pmatrix} \alpha_{xx} & 0 & 0 \\ 0 & \alpha_{xx} & 0 \\ 0 & 0 & \alpha_{zz} \end{pmatrix}$$

3. The components of α

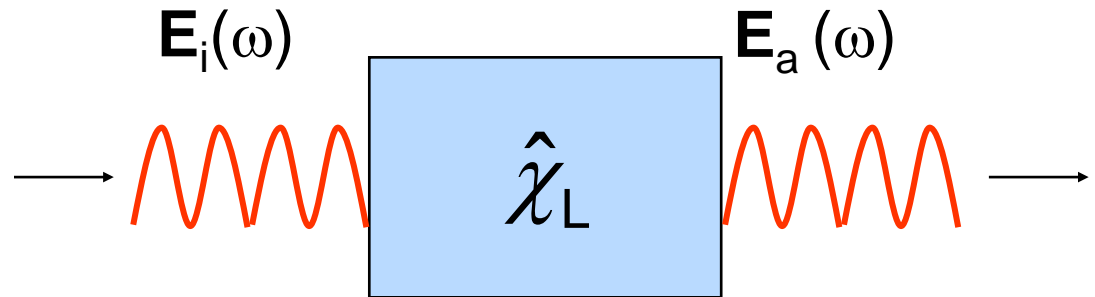
$m = 2$	xx	yy	zz	xy	yx	$xz(2)$	$yz(2)$
K_2	xx	xx	zz	xy	$-xy$	0	0
L_2	xx	xx	zz	0	0	0	0
M_2	0	0	0	xy	$-xy$	0	0

Part II – Nonlinear Optics

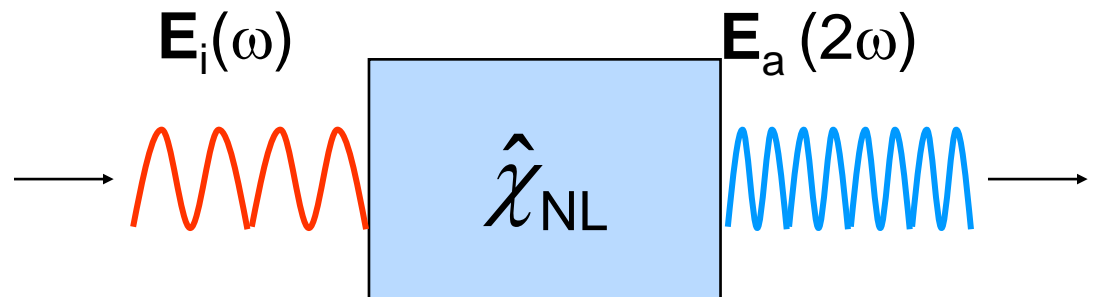
- Introduction & overview
- Second harmonic generation (SHG)
- Determination of tensor components
- SHG & (multi-)ferroic order

Nonlinear Optics

Linear optics:



Nonlinear optics:



Nonlinear Optics

$$P_i(\omega) \propto \underbrace{\chi_{ij}^{(1)} E_j(\omega_1)}_{\text{PL}} + \underbrace{\chi_{ijk}^{(2)} E_j(\omega_1) E_k(\omega_2) + \chi_{ijkl}^{(3)} E_j(\omega_1) E_k(\omega_2) E_l(\omega_3) + \dots}_{\text{PNL}}$$

Quadratic effects: Frequency doubling $\omega = 2\omega_1$

Pockels effect $P_i(\omega) \propto \chi_{ijk}^{(2)} E_j(\omega) E_k(0)$

Cubic effects: Sum frequency generation $\omega = \omega_1 + \omega_2 + \omega_3$

Difference frequency $\omega = 2\omega_1 - \omega_2$

But: $\chi^{(1)} \approx 1$, $\chi^{(2)} \approx 10^{-10}$ cm / V, $\chi^{(3)} \approx 10^{-17}$ cm² / V²

Conventional light sources $E \approx 1$ V/cm

⇒ Laser

First Observation of Optical Harmonic Generation

P. A. Franken, A. E. Hill, C. W. Peters, and G. Weinreich

Generation of Optical Harmonics

Phys. Rev. Lett. 7, 118 (1961)

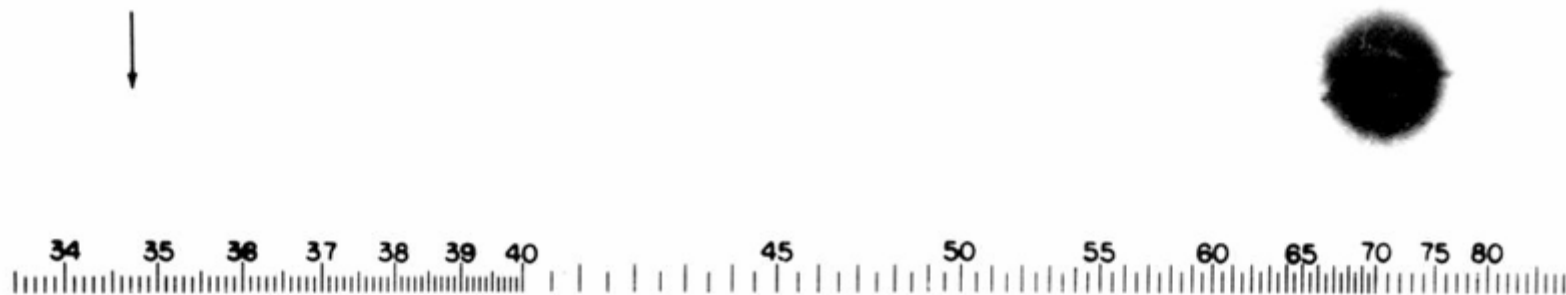
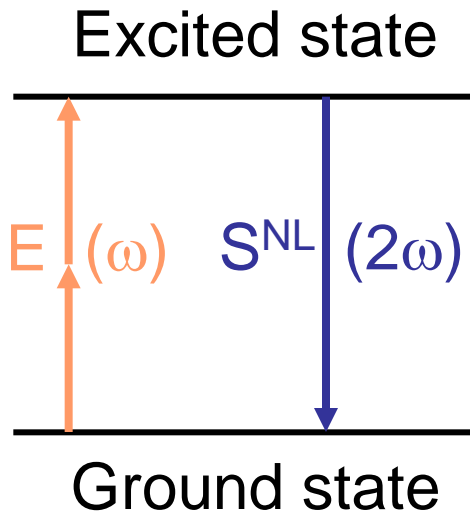


FIG. 1. A direct reproduction of the first plate in which there was an indication of second harmonic. The wavelength scale is in units of 100 Å. The arrow at 3472 Å indicates the small but dense image produced by the second harmonic. The image of the primary beam at 6943 Å is very large due to halation.

Optical Second Harmonic Generation (SHG)



SH-source term:

$$S^{NL}(2\omega) \propto P^{NL}(2\omega) \propto \chi(2\omega)E(\omega)E(\omega)$$

SH intensity:

$$I_{SH} \propto |S^{NL}|^2 \propto |\chi EE|^2 = |\chi|^2 I_0^2$$

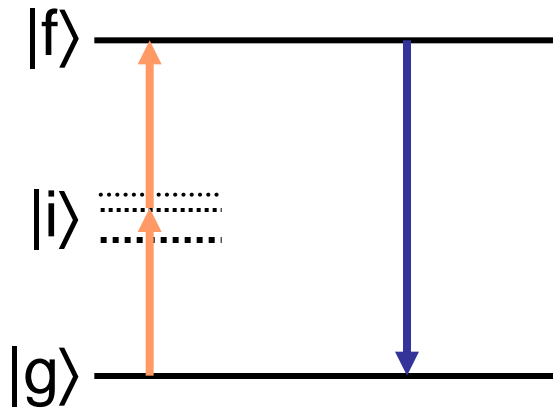
$P^{NL}(2\omega)$, $E(\omega)$: polar tensors of first rank

$\Rightarrow \chi(2\omega)$ polar tensor of third rank



No SHG in centrosymmetric crystals!

The Nonlinear Susceptibility χ



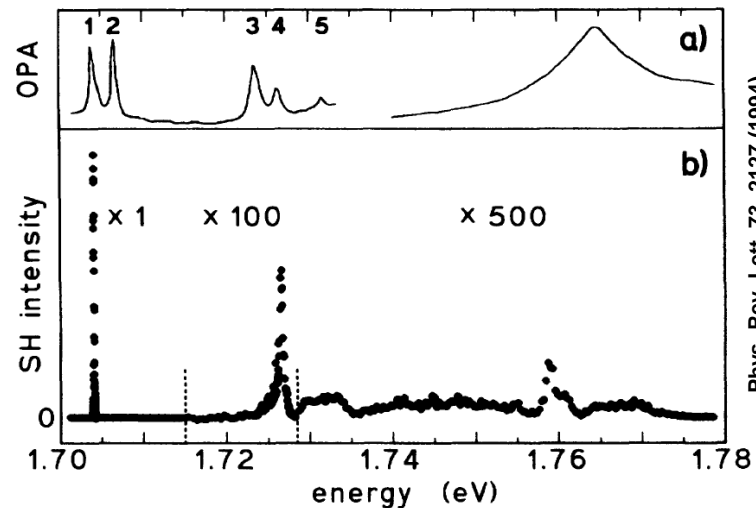
For SHG follows from perturbation theory:

$$\hat{\chi}(2\omega) \propto \sum_{i,f} \frac{\langle g | \hat{H}(2\hbar\omega) | f \rangle \langle f | \hat{H}(\hbar\omega) | i \rangle \langle i | \hat{H}(\hbar\omega) | g \rangle}{(E_f - E_g - 2\hbar\omega)(E_i - E_g - \hbar\omega)}$$

States $\langle i |$ are real states that are excited with large energy mismatch: $\Delta E \cdot \Delta t \sim \hbar$

SHG is a coherent, resonant process!

e.g. SHG spectra of antiferromagnetic Cr_2O_3



Phys. Rev. Lett. 73, 2127 (1994)

Nonlinear Multipole Contributions

Light-matter interaction Hamiltonian:

$$\hat{H} \propto \vec{p} \cdot \vec{A} \quad \text{with} \quad \vec{A} = \sum_{\vec{k}} \vec{A}_{\vec{k}} e^{i\vec{k}\vec{r}} + \text{c.c.}$$

\vec{p} : Electron impulse operator, \vec{A} : Light field vector potential

In crystals usually $\lambda \propto |\vec{k}|^{-1} \gg a$ (= lattice constant)

$$\Rightarrow \exp(i\vec{k}\vec{r}) \cong 1 + i\vec{k}\vec{r} + \dots \quad \Rightarrow \quad \hat{H} = \underbrace{\hat{H}_{\text{ED}}}_{\text{Zero order}} + \underbrace{\hat{H}_{\text{MD}} + \hat{H}_{\text{EQ}}}_{\text{First order}}$$

Nonlinear Multipole Contributions

Three nonlinear contributions:

Electric dipole (ED): $\vec{P}^{\text{NL}}(2\omega) \propto \chi^{\text{ED}}(2\omega)\mathbf{E}(\omega)\mathbf{E}(\omega)$

Magnetic dipole (MD): $\vec{M}^{\text{NL}}(2\omega) \propto \chi^{\text{MD}}(2\omega)\mathbf{E}(\omega)\mathbf{E}(\omega)$

Electric quadrupole (EQ): $\hat{Q}^{\text{NL}}(2\omega) \propto \chi^{\text{EQ}}(2\omega)\mathbf{E}(\omega)\mathbf{E}(\omega)$

⇒ Multipole expansion of source term \vec{S} for SHG:

$$\vec{S} = \underbrace{\mu_0 \frac{\partial^2 \vec{P}^{\text{NL}}}{\partial t^2}} + \mu_0 \left(\vec{\nabla} \times \frac{\partial \vec{M}^{\text{NL}}}{\partial t} \right) - \mu_0 \left(\vec{\nabla} \frac{\partial^2 \hat{Q}^{\text{NL}}}{\partial t^2} \right)$$

Leading contribution of the order α larger,
but maybe symmetry forbidden!

SHG in (Multi-)ferroics

Sa et al. Eur. Phys. J. B 14 (2000):

$$\chi^{\text{SHG}}(T < T_0) = \chi(T > T_0) \circlearrowright$$

Order parameter

Susceptibility in the para phase

Susceptibility in the ferroic phase

- χ^{SHG} is a function of the order parameter \circlearrowright
- Non-zero components of χ^{SHG} obtained from symmetry of the order parameter and the crystal in the para phase
→ **Curie's principle**

Order Parameter \odot

Properties:

- Zero for $T > T_0$, non-zero for $T < T_0$
- Invariant under symmetries of the group of the ordered phase
- Non-invariant under the symmetries lost at the phase transition
- Each orientation of \odot represents one ferroic domain state

Here:

\odot is the lowest rank tensor that fulfils all of the properties above

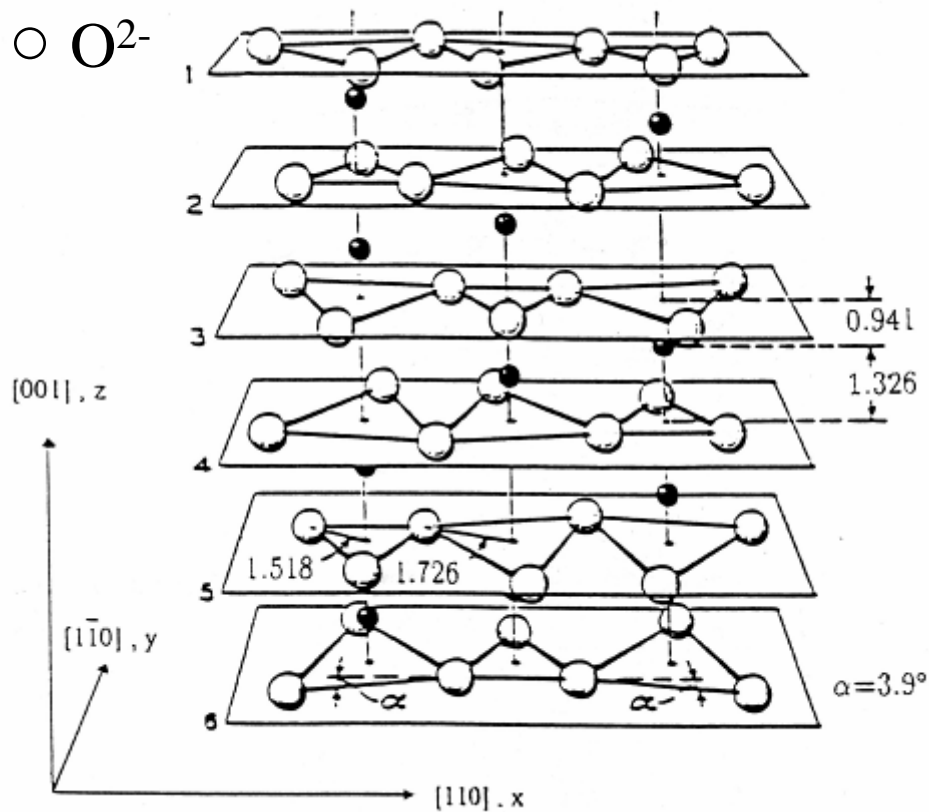
e.g. the polarization \mathbf{P} in a ferroelectric or magnetization \mathbf{M} in ferromagnetic crystal

Antiferromagnetic Cr_2O_3

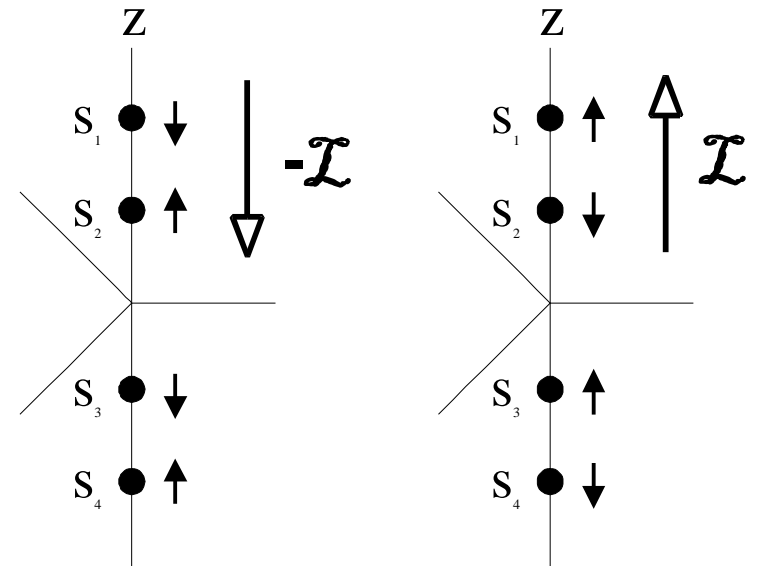
Crystallographic point group $\bar{3}m$

• Cr^{3+}

○ O^{2-}



Magnetic point group $\bar{3}m$



Order parameter:

$$\mathcal{L}_Z = s_{1,z} - s_{2,z} + s_{3,z} - s_{4,z}$$

Antiferromagnetic Cr_2O_3

Properties of orderparameter \mathcal{L}_z :

- Symmetry $\bar{3}m$
- c-axial scalar

$$\Rightarrow \chi_{ijk}^{\text{SHG}}(T < T_N) = \chi_{ijk}(T > T_N)\mathcal{L}_z$$

i-axial, third rank: $\chi_{yyy} = -\chi_{yxx} = -\chi_{xyx} = -\chi_{xxy}$

$$\text{c-axial, third rank: } \chi_{yyy} = -\chi_{yxx} = -\chi_{xyx} = -\chi_{xxy}$$

Antiferromagnetic Cr_2O_3

Tensor components: $\chi_{yyy} = -\chi_{yxx} = -\chi_{xyx} = -\chi_{xxy}$

$$\Rightarrow P(2\omega) \propto \begin{pmatrix} 2\chi_{yyy}(2\omega)E_x(\omega)E_y(\omega) \\ \chi_{yyy}(2\omega)(E_x^2(\omega) - E_y^2(\omega)) \\ 0 \end{pmatrix}$$

k-direction & polarization selection rules:

1. $k||x$: Only signal for $E||y$ & $P||y$
2. $k||y$: No signal
3. $k||z$: All components allowed

Set of yes or no type rules to determine symmetry and structure

Generalized Description

Higher order contributions of \mathcal{O} :

$$\chi(T < T_0) = \chi_0(T > T_0) + \chi_1(T > T_0)\mathcal{O} + \chi_2(T > T_0)\mathcal{O}\mathcal{O} + \dots$$

Multiple order parameters $\mathcal{O}_1, \mathcal{O}_2, \dots$ ($T_{01} < T_{02} < \dots$):

$$\begin{aligned}\chi(T < T_{01}) &= \chi_0(T > T_{01}) + \chi_1(T > T_{01})\mathcal{O}_1 + \dots \\ &= \chi_{00}(T > T_{02}) + \chi_{01}(T > T_{02})\mathcal{O}_2 + \dots \\ &\quad + \chi_{10}(T > T_{02})\mathcal{O}_1 + \chi_{11}(T > T_{02})\mathcal{O}_2\mathcal{O}_1 + \dots \\ &\quad \vdots\end{aligned}$$

Analogue contributions for ED, MD and EQ:

Up to 12 χ -tensors for two order parameter compounds!

SHG in a Multiferroic Compound

ED contribution for magnetic ferroelectrics:

$$\vec{P}^{\rightarrow NL}(2\omega) = \varepsilon_0 [\hat{\chi}(0) + \hat{\chi}(\wp) + \hat{\chi}(\ell) + \hat{\chi}(\wp\ell) + \dots] \vec{E}(\omega) \vec{E}(\omega)$$

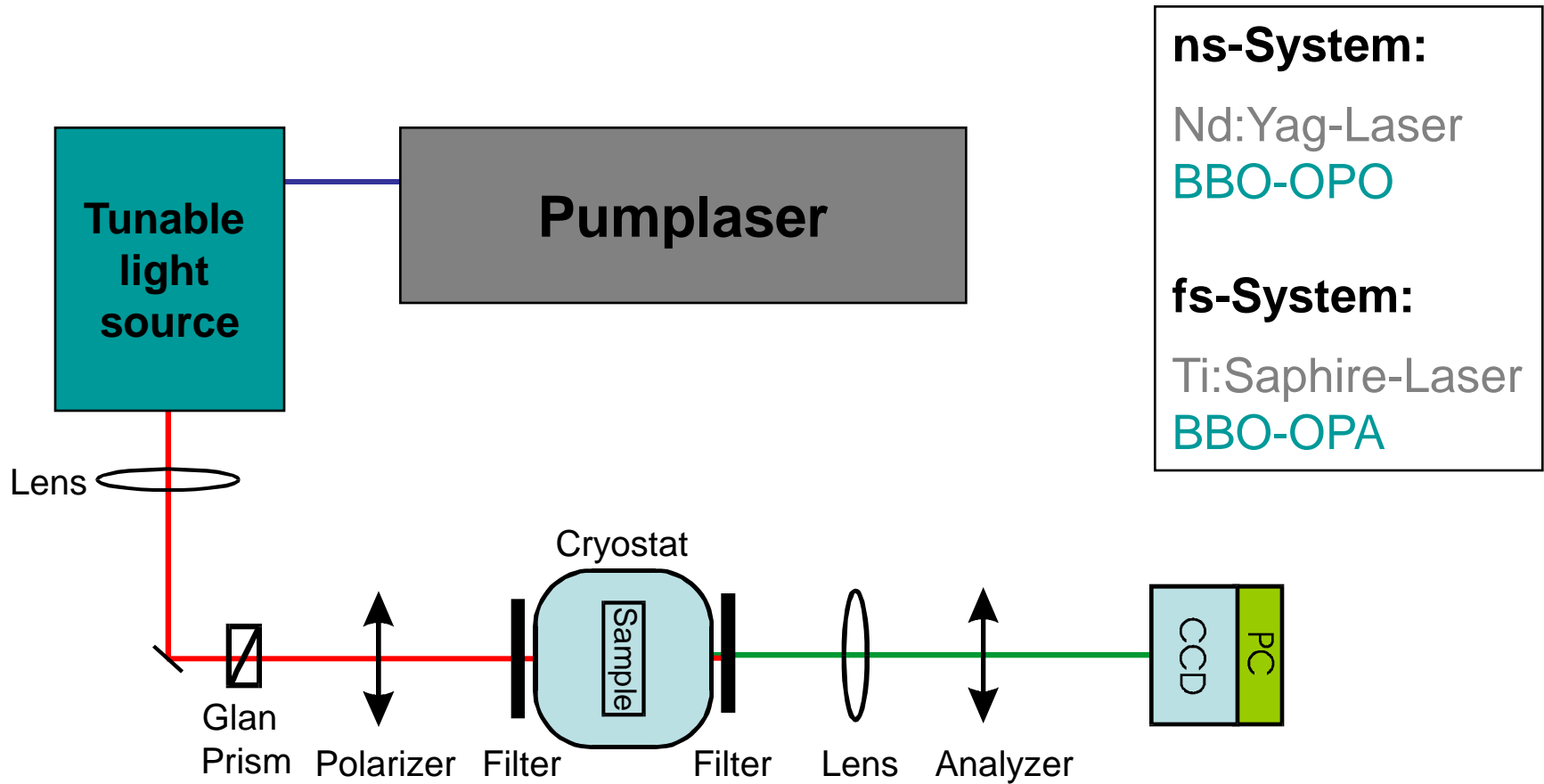
$\chi(0)$:	Paraelectric paramagnetic contribution	—	always allowed
$\chi(\wp)$:	(Anti)ferroelectric contribution	} [allowed below the respective ordering temperature
$\chi(\ell)$:	(Anti)ferromagnetic contribution		
$\chi(\wp\ell)$:	Magnetolectric contribution		

- SHG allows simultaneous investigation of magnetic and electric structures
- Selective access to electric and magnetic sublattices
- Ferroelectromagnetic contribution reveals the magneto-electric interaction between the sublattices

Part III - Experimental Techniques

- Spectral sensitivity
- Freedom of k-direction and light polarizations
- Temperature variation
- External magnetic and electric fields
- Optical phase sensitivity
- Spatial resolution
- Transmission & Reflection measurements
- Surface & interface sensitivity
- Time resolution

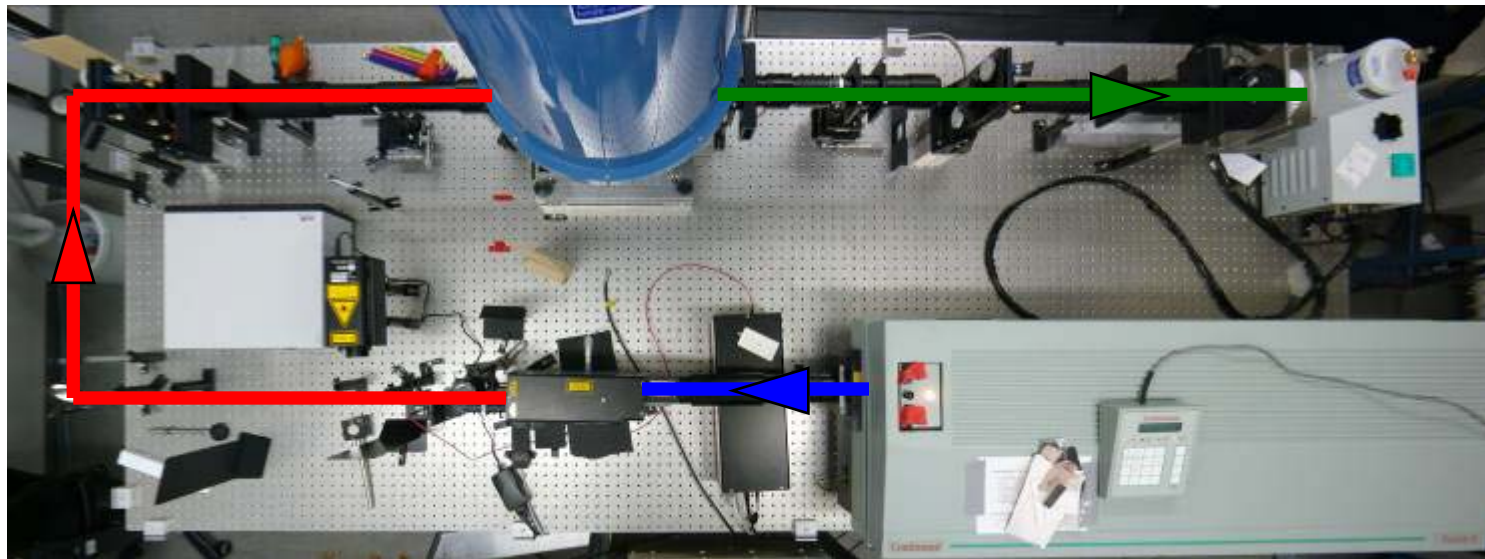
Basic Experimental Setup



Spectroscopy & Imaging Setup

Magnet
cryostat

CCD camera

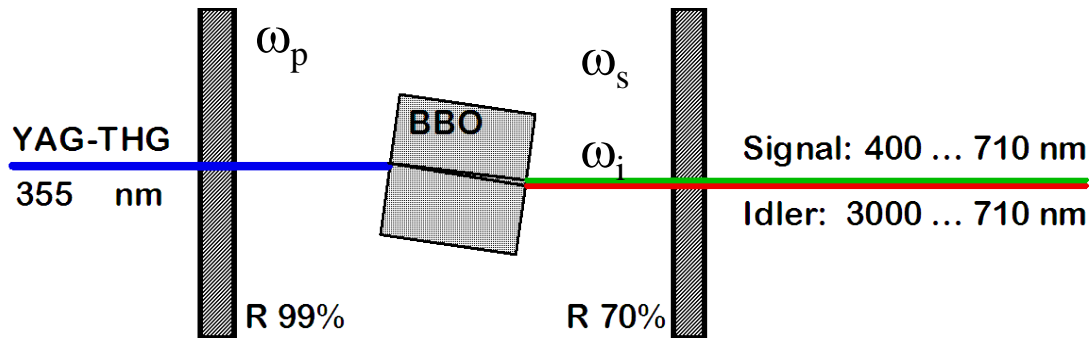


BBO-OPO

Nd:YAG laser

Optical Parametric Oscillator

Passive tuneable laser light source in the range 400nm - 3000nm



Parametric oscillation of transparent nonlinear crystal with high $\chi^{(2)}$ -coefficients (here: beta-barium-borate β -BaB₂O₄)

Conservation of energy:

$$\hbar\omega_p = \hbar\omega_s + \hbar\omega_i \quad \rightarrow \quad \omega_p = \omega_s + \omega_i$$

Conservation of momentum:

$$\hbar k_p = \hbar k_s + \hbar k_i \quad \rightarrow \quad n_p \omega_p = n_s \omega_s + n_i \omega_i$$

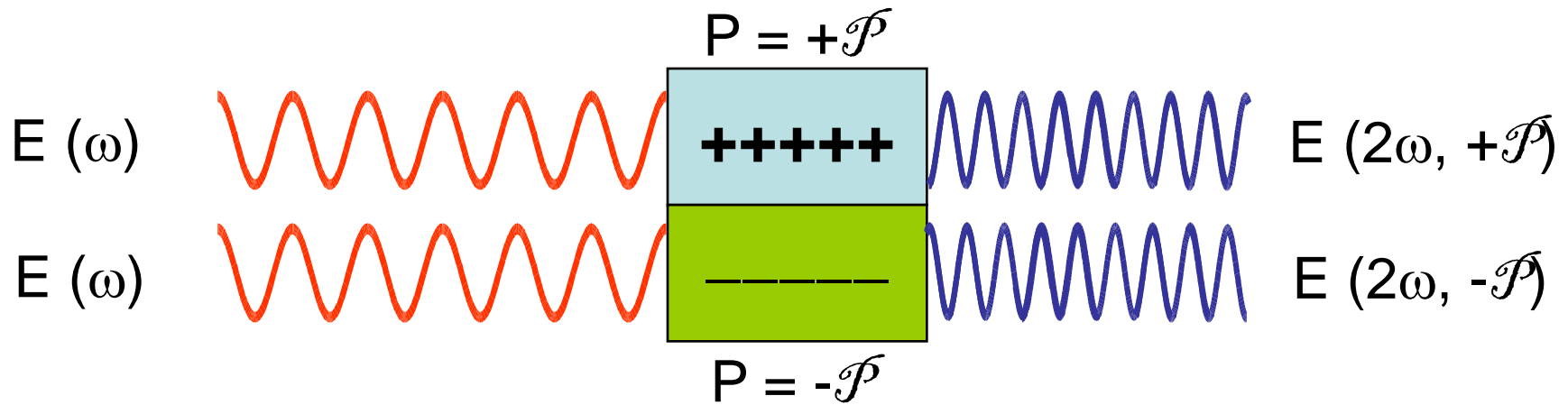
n – refractive index \rightarrow frequency tuning by rotation of crystal

Part III - Experimental Techniques

Nonlinear optical phase measurements

Domain Imaging

Example: Ferroelectric 180° domains:

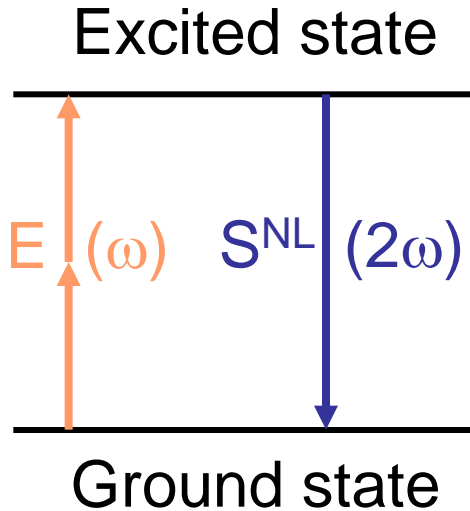


$$\left. \begin{aligned} E(2\omega, +\mathcal{P}) &\propto \chi(+\mathcal{P}) E(\omega)E(\omega) = +\chi(|\mathcal{P}|)E(\omega)E(\omega) \\ E(2\omega, -\mathcal{P}) &\propto \chi(-\mathcal{P}) E(\omega)E(\omega) = -\chi(|\mathcal{P}|) E(\omega)E(\omega) \end{aligned} \right\} \text{180° Phase difference!}$$



Domains distinguishable by the phase of the nonlinear signal.

Phase Sensitive Measurements



SH-source term:

$$S^{\text{NL}}(2\omega) \propto \chi(2\omega)E(\omega)E(\omega)$$

SH intensity:

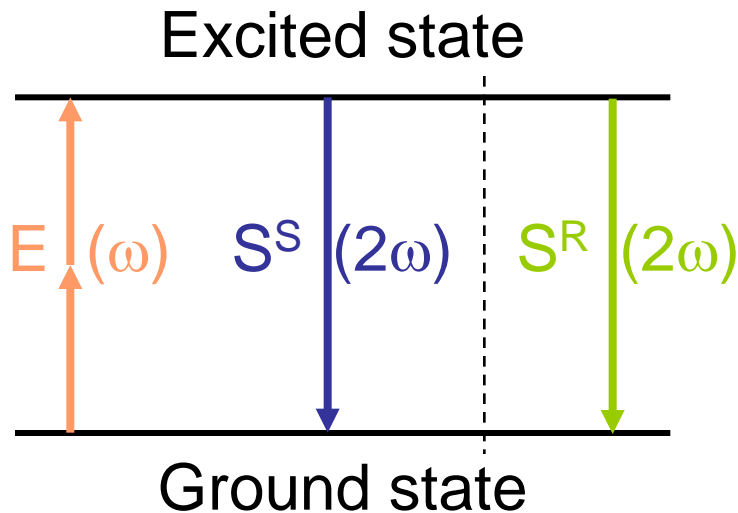
$$I_{\text{SH}} \propto |S^{\text{NL}}|^2 \propto |\chi EE|^2 = |\chi|^2 I_0^2$$

Problem: Only direct measurement of intensity

⇒ No direct access to the phase!

Solution: Interference measurements

Phase Sensitive Measurements



Sample source term:

$$S^S(2\omega) \propto \chi^S(2\omega) E(\omega)E(\omega)$$

Reference source term:

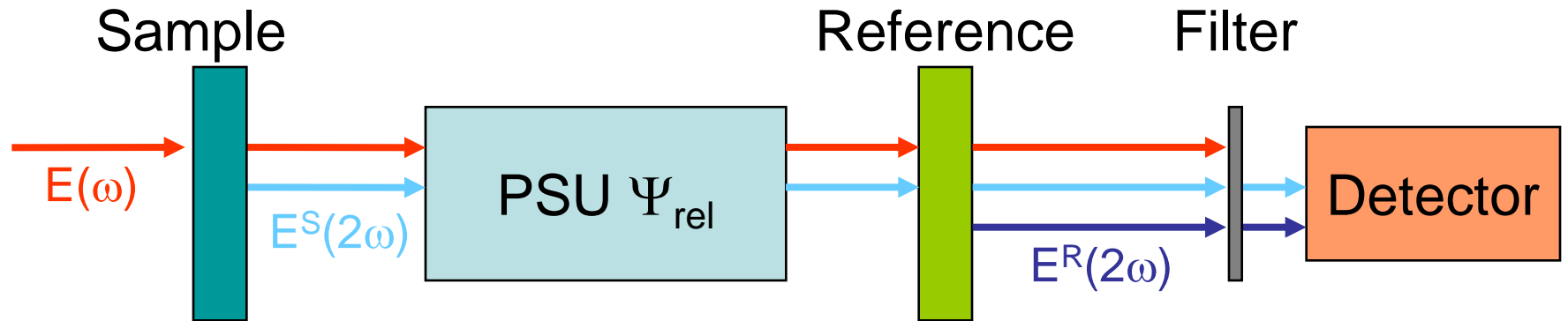
$$S^R(2\omega) \propto \chi^R(2\omega) E(\omega)E(\omega)$$

Total intensity: $I_{SH} \propto |S^S + S^R|^2 \propto |\chi^S + Ae^{i\psi} \chi^R|^2 I_0^2$

$$= \underbrace{(|\chi^S|^2 + |A\chi^R|^2)}_{\text{always } > 0} + \underbrace{2\chi^S \chi^R \cos \psi}_{\text{interference term}} I_0^2(\omega)$$

Experimental access to amplitude A and phase ψ !

Experimental Realisation



PSU = Phase Shifting Unit:

Induces phase shift Ψ_{rel} between $E(\omega)$ and $E^S(2\omega)$ and therefore between $E^S(2\omega)$ and $E^R(2\omega)$

Experimental realisation:

- Gas pressure cell
- Rotated glass plates or shifted glass wedges
- Distance variation

Experimental Realisation

Measuring SH-intensity I as function of Ψ_{rel} :

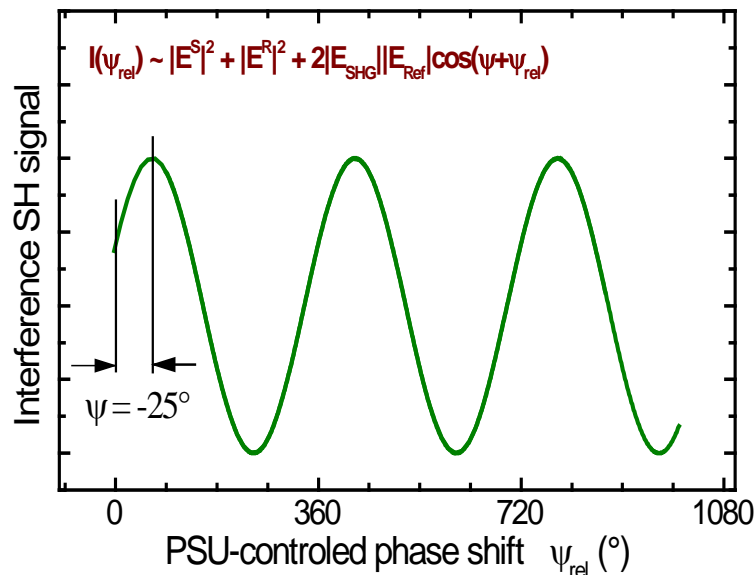
$$I(\Psi_{\text{rel}}) \propto |\mathbf{E}^{\text{S}} + \mathbf{E}^{\text{R}}|^2 = |\mathbf{E}^{\text{S}}|^2 + |\mathbf{E}^{\text{R}}|^2 + 2 |\mathbf{E}^{\text{S}}| |\mathbf{E}^{\text{R}}| \cos(\Psi + \Psi_{\text{rel}})$$

with $\Psi = \Psi^{\text{S}} + \Psi^{\text{R}} + \Psi_0$

(Ψ_0 by PSU and distance
sample \leftrightarrow reference)

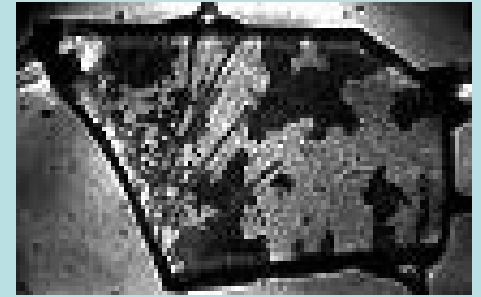
For $\Psi_0 \rightarrow 0$ and if Ψ^{R} known:

Absolute measurement of Ψ^{S}



Spatially resolved:

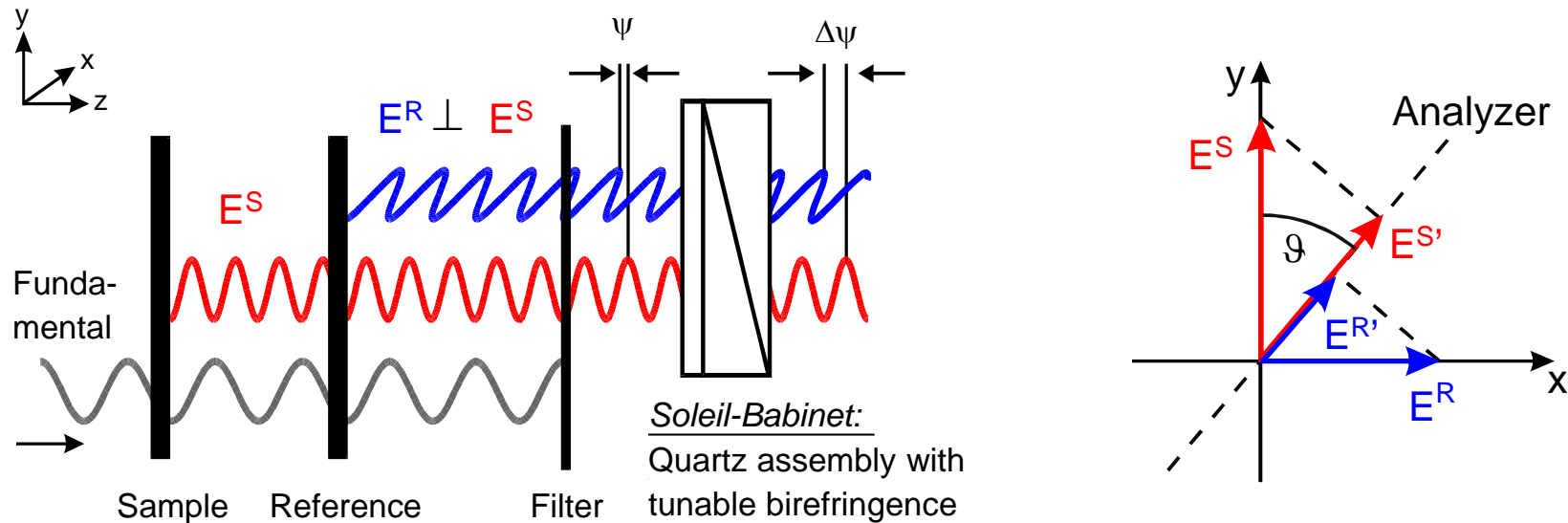
e.g. AFM domain
in YMnO_3



Disadvantages of the Standard Methods

- Only measurements with external reference (⚡ multiferroics)
- Distance sample \leftrightarrow reference reduces image quality
- Loss of coherence due to large sample \leftrightarrow reference distance \Rightarrow weak interference signal
- Mechanical/optical instabilities due to moving parts

Phase Resolved SH Imaging



Soleil-Babinet compensator as PSU behind sample & reference:

⇒ Sample ↔ reference distance can be reduced to zero

⇒ Measurements with external or *internal* reference

E^S and E^R are projected on common direction via an analyzer:

⇒ Optimization of signal contrast

Soleil-Babinet Compensator

Quartz assembly made of
two wedged crystals (2a, 2b)
+ a compensation crystal

Phase shift Ψ :

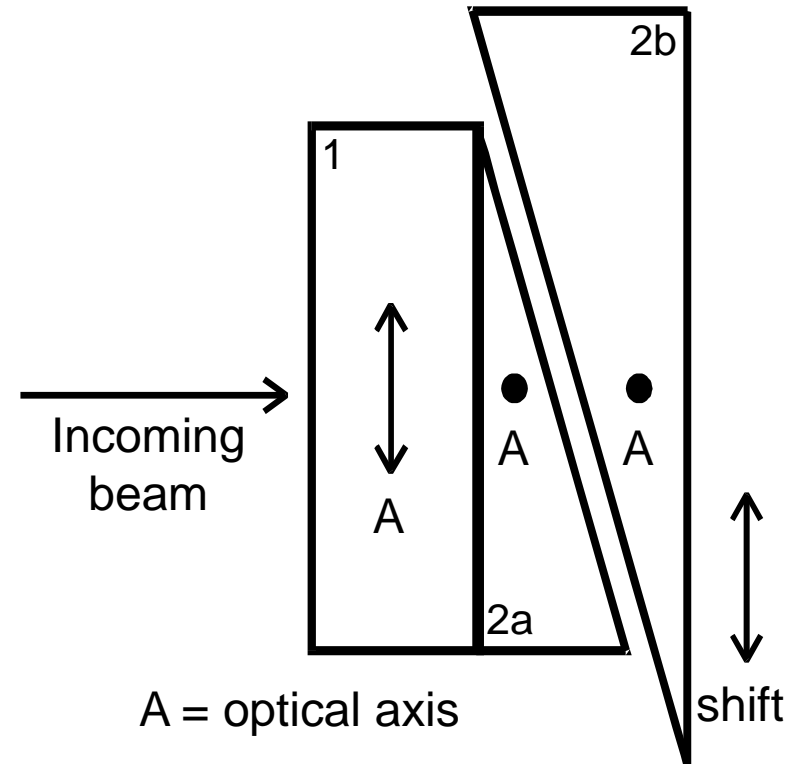
$$\Psi = \frac{2\pi}{\lambda} (d_2 - d_1) \Delta n$$

d_1 : Thickness compensation crystal

d_2 : Total thickness of the wedges

λ : Wavelength

$\Delta n = n_e - n_o$: Refractive index mismatch

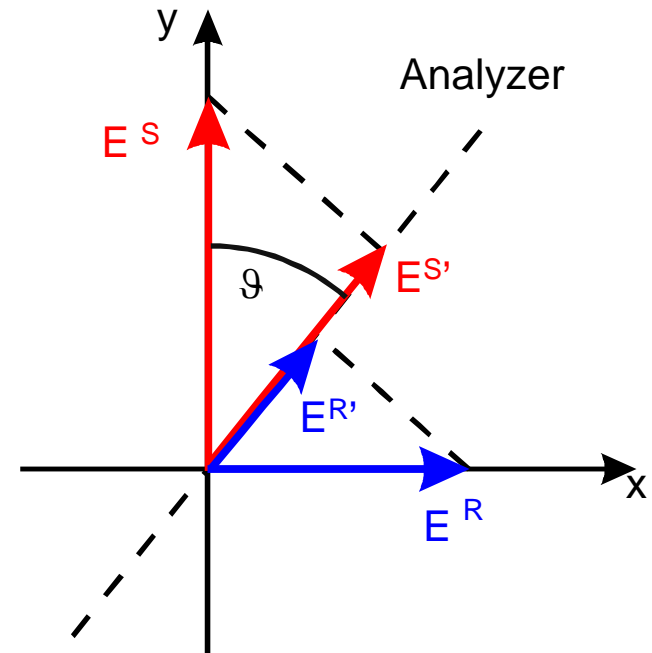


Signal Optimization

$$\left. \begin{aligned} \vec{E}^R &= E_0^R e^{i\Psi^R} \vec{e}_x \\ \vec{E}^S &= E_0^S e^{i\Psi^S} \vec{e}_y \end{aligned} \right\} \Rightarrow \begin{cases} E^{R'}(\vartheta) = E_0^R e^{i\Psi^R} \sin \vartheta \\ E^{S'}(\vartheta) = E_0^S e^{i\Psi^S} \cos \vartheta \end{cases}$$

Interference:

$$\begin{aligned} I(\vartheta) &= |E^{R'}(\vartheta) + E^{S'}(\vartheta)|^2 = \\ &= |E_0^R \sin \vartheta|^2 + |E_0^S \cos \vartheta|^2 + 2|E_0^R||E_0^S| \sin \vartheta \cos \vartheta \cos(\Psi^R - \Psi^S) \end{aligned}$$

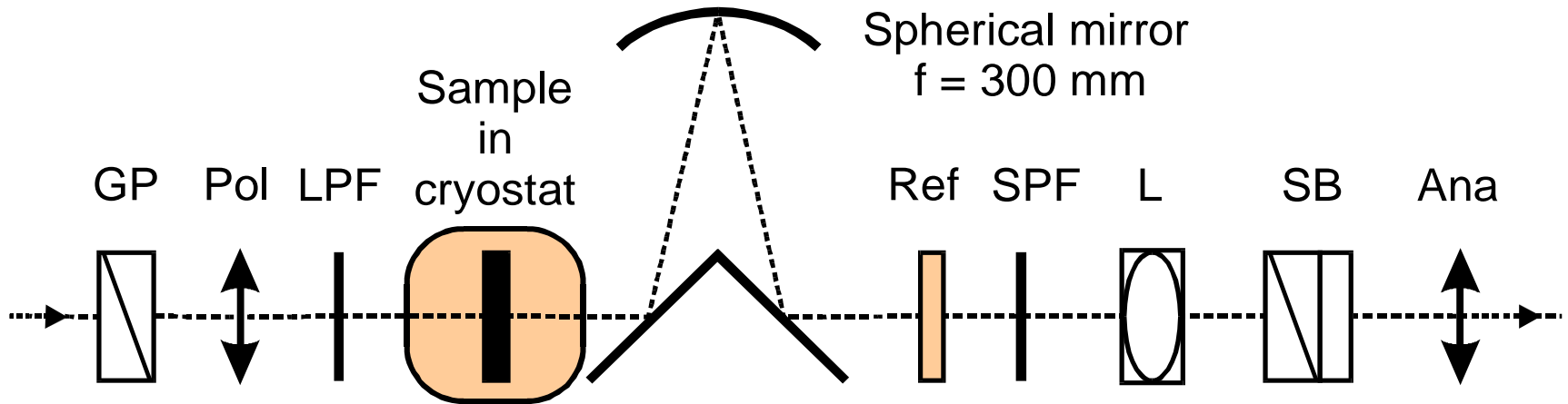


$$\text{Contrast: } C = \frac{I_{\max}}{I_{\min}} = 1 \dots \infty$$

$$\text{Visibility: } V = \frac{I_{\max} - I_{\min}}{I_{\max} + I_{\min}} = 0 \dots 1$$

Maximum for
 $E^{R'}(\vartheta_0) = E^{S'}(\vartheta_0)$

Phase Resolved SH Imaging (Setup)



- Measurements with external or internal reference
- Reference outside cryostat
⇒ high degree of experimental freedom
- Achromatic beam imaging for improved image quality and compensation of loss of (spatial) coherence

Coherence Effects

Interference including the effect of coherence:

$$I(\Psi) = I_1 + I_2 + 2\sqrt{I_1 I_2} |\gamma| \cos(\Psi_0 + \Psi)$$

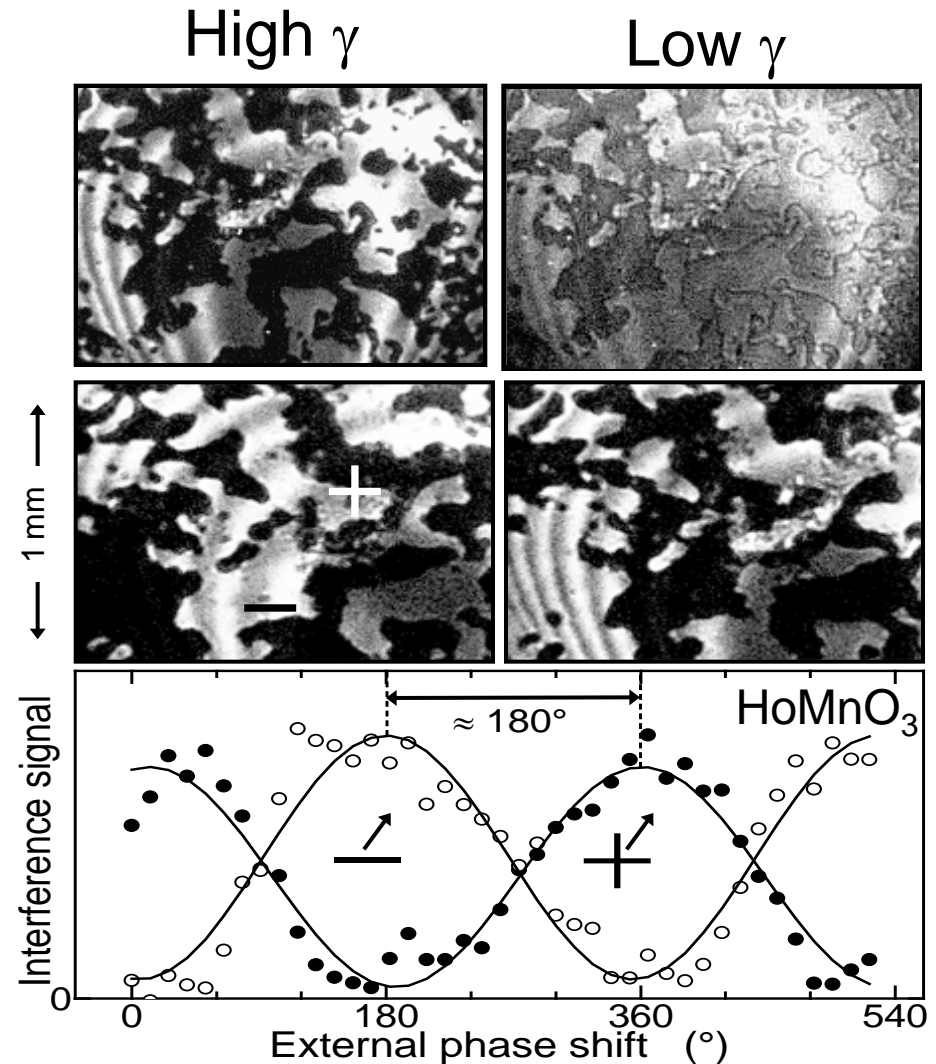
Coherence: $|\gamma|$

Visibility:

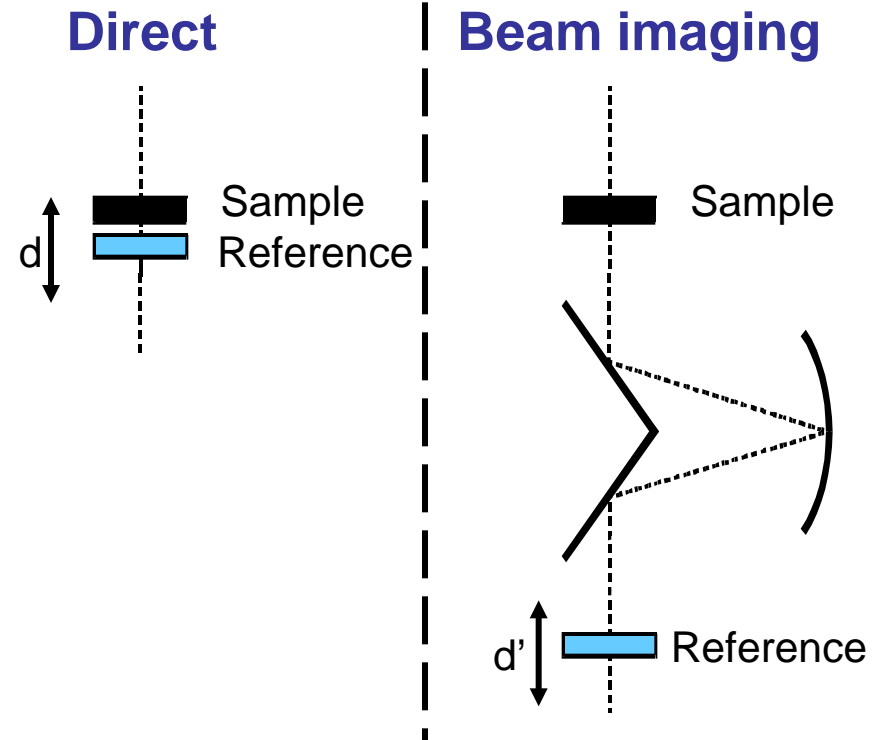
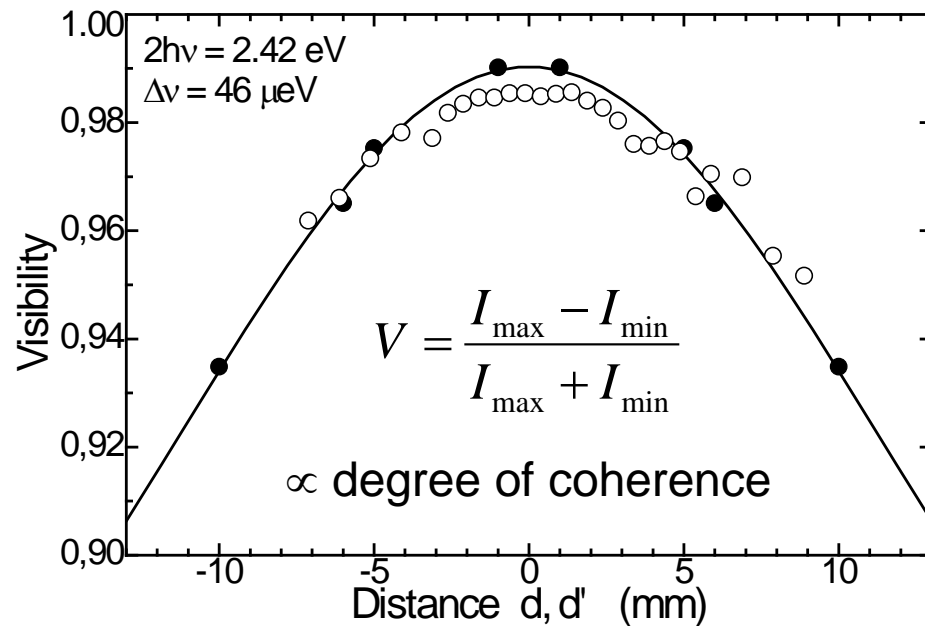
$$V = \frac{I_{max} - I_{min}}{I_{max} + I_{min}} = \frac{2\sqrt{I_1 I_2} |\gamma|}{I_1 + I_2}$$

For $I_1 = I_2 \Rightarrow V = |\gamma|$

$|\gamma| > 99\%$ possible!



Phase-Resolved SH Imaging (Results)



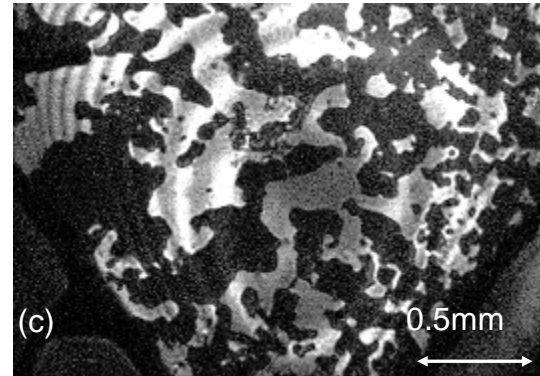
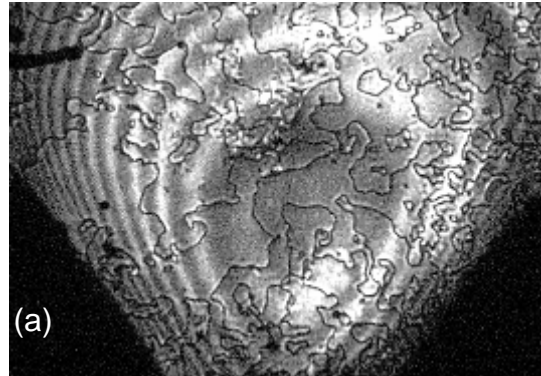
Visibility
almost 100%



Loss of (spatial)
coherence
fully compensated!

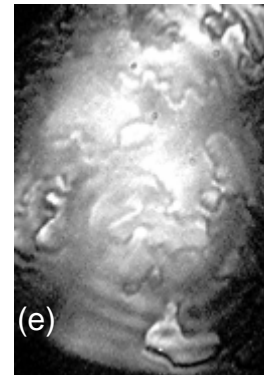
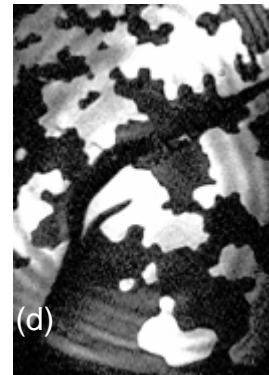
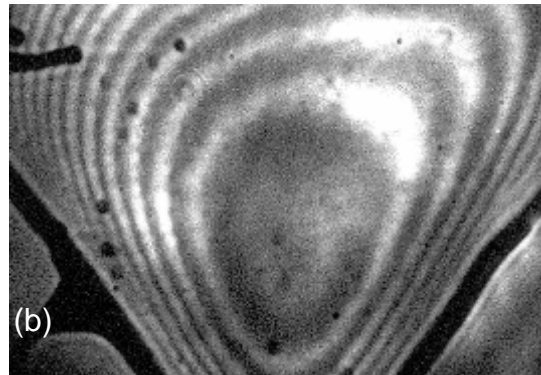
Phase-Resolved SH Imaging (Results)

Sample



Sample
+
Reference

Reference



imaging

direct

Phase-Resolved SH Imaging (Summary)

- Large working distances (~ 1 m)
- More experimental freedom
- High signal contrast
- Improved image quality
- Allows use of broadband laser sources with poor beam quality

Part III - Experimental Techniques

Nonlinear imaging & the problem of optical resolution

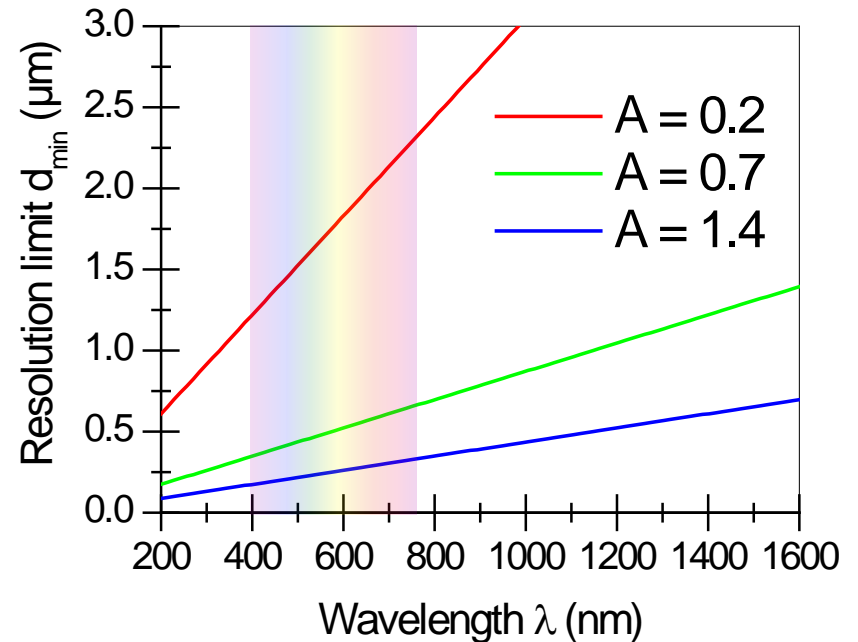
Limit of Optical Resolution

Optical resolution is limited by diffraction:

$$d_{\min} = 0.61 \frac{\lambda}{A} \quad \text{with numerical aperture } A = n \sin \varphi$$

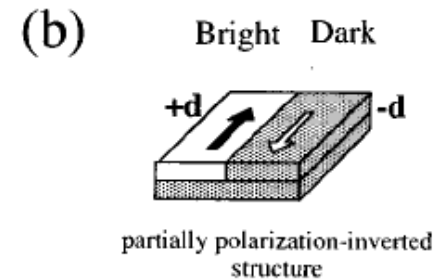
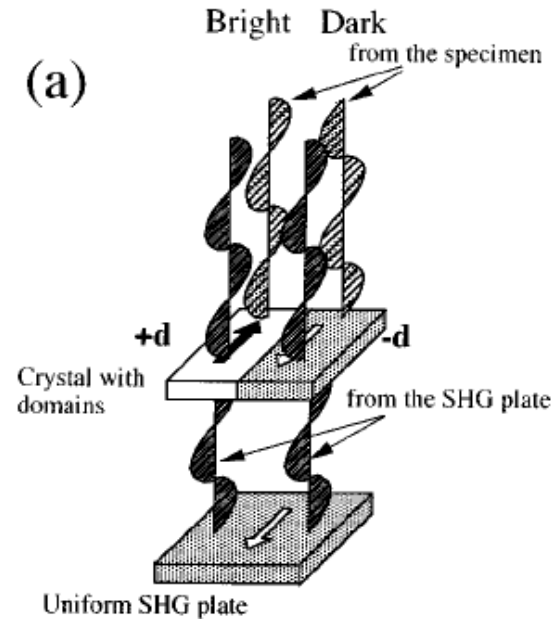
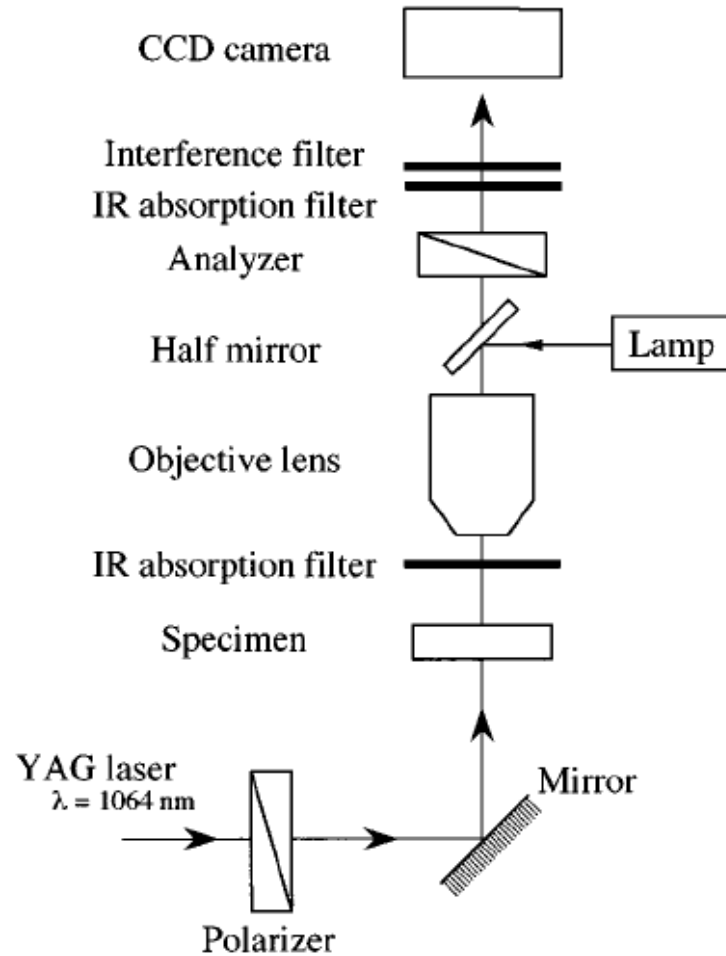
Typical values of A:

- Standard lens
($f=200\text{mm}$, $\varnothing=50\text{mm}$): $A \approx 0.2$
- Photo lens: $A \approx 0.7$
- Microscope objective
up to $A = 1.4$



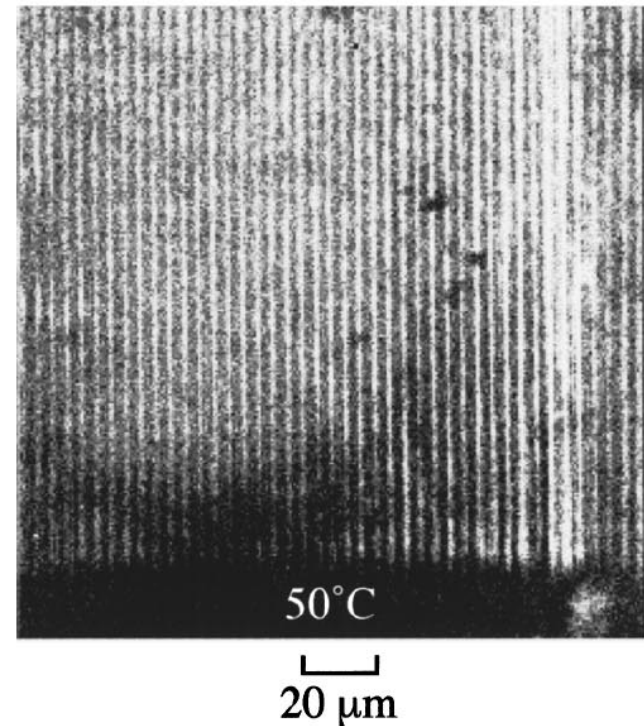
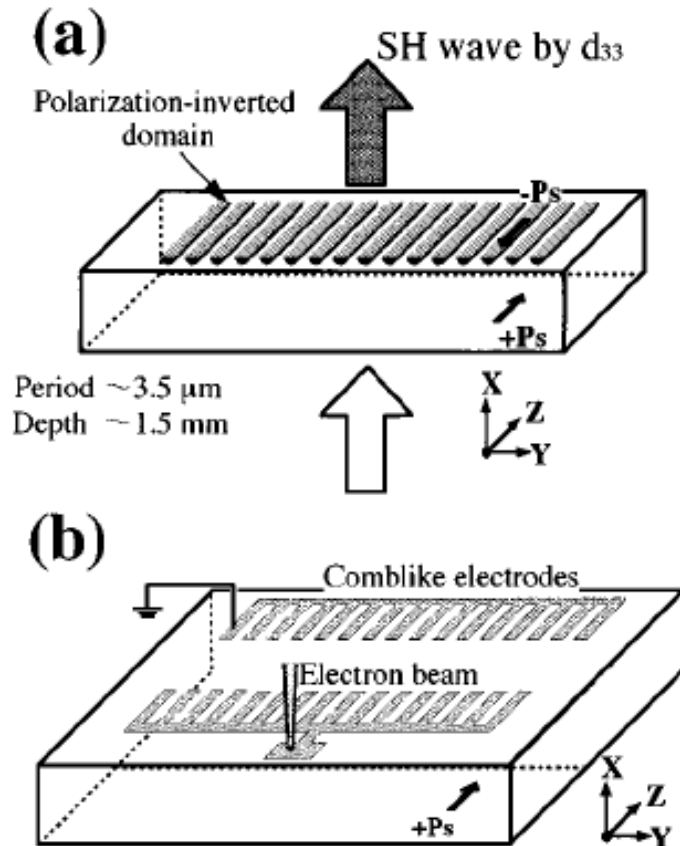
⇒ Resolution limit down to some hundred nm

SHG Microscopy



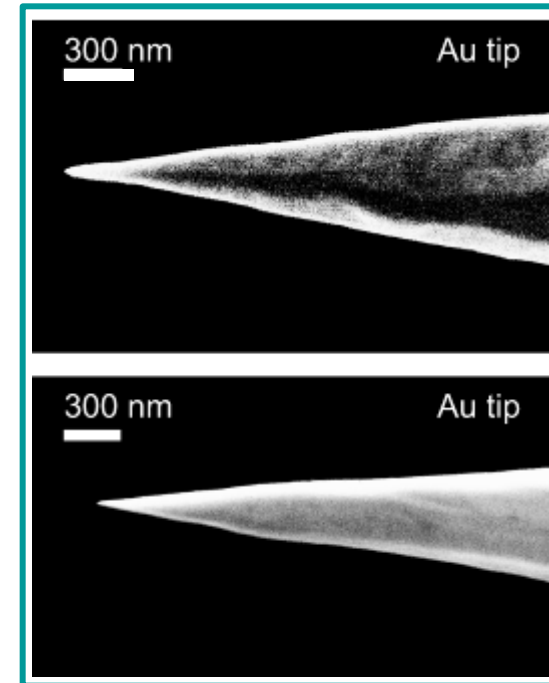
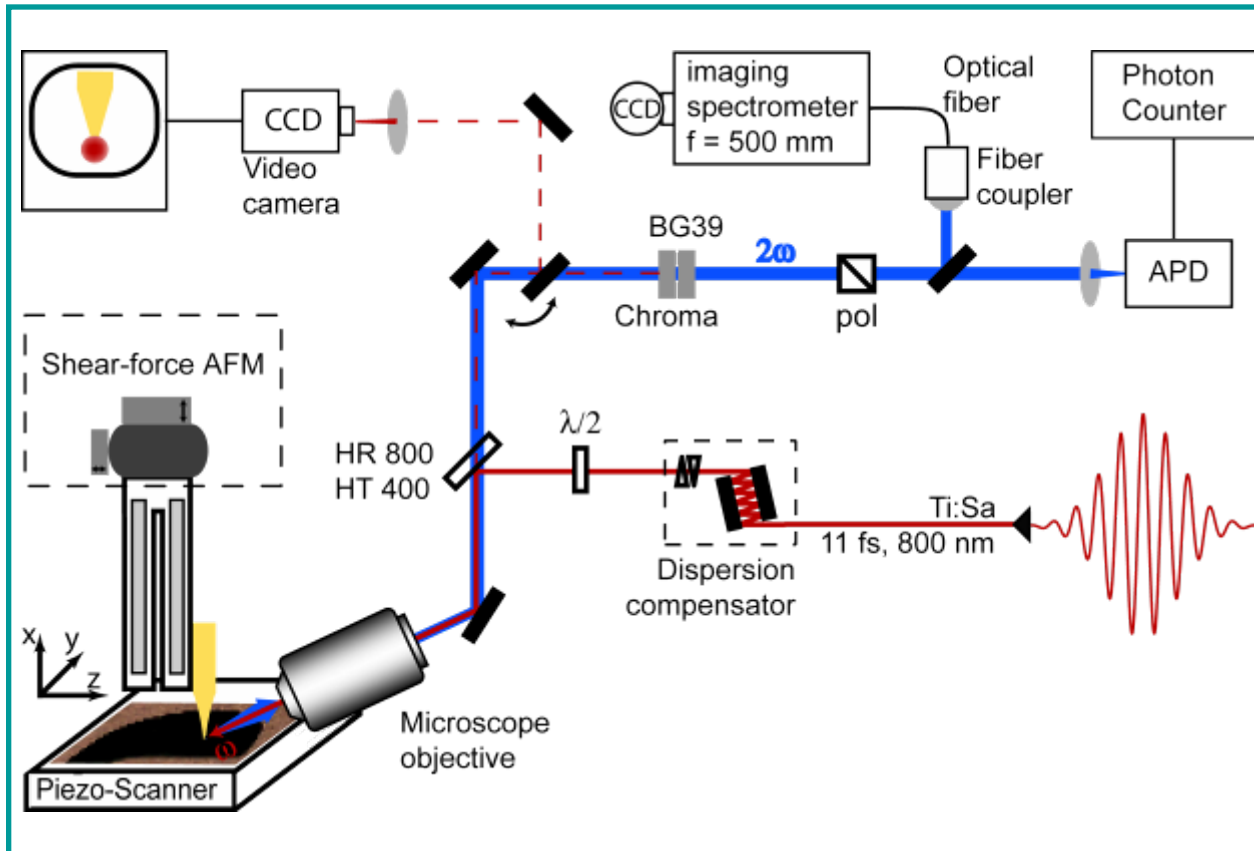
SHG Microscopy

Ferroelectric stripe domains in a LiTaO_3 QPM device



Going Beyond the Optical Resolution Limit

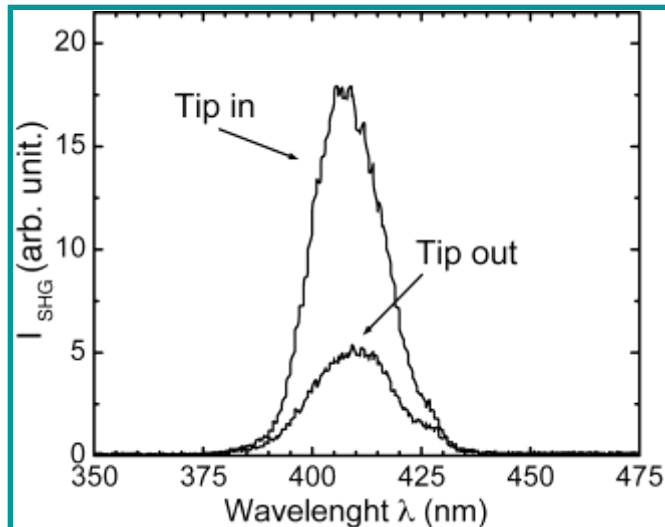
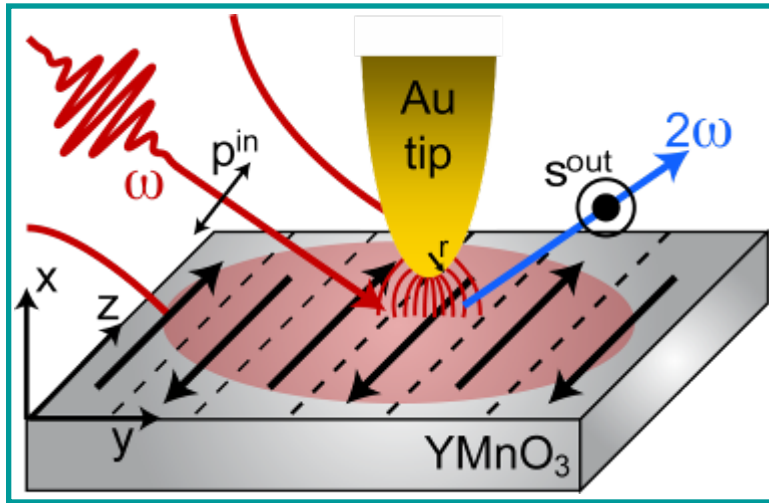
Tip- enhanced near-field microscope



SEM micrographs of Au tips: $R \sim 10$ nm

[Neacsu, Reider, and Raschke, Phys. Rev. B **71**, 201402 (2005)]

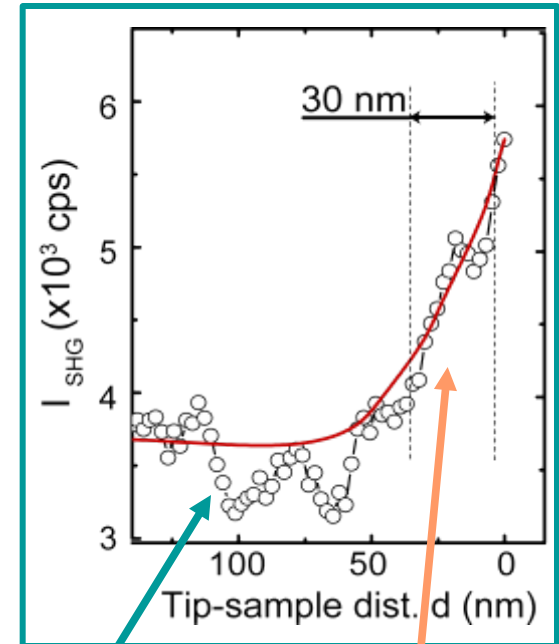
Imaging of FEL Domains in YMnO_3



$$\vec{E}(\omega) = (E_x(\omega), E_y(\omega), 0)$$

$$P_z^{(2)}(2\omega) \approx \chi_{zx}^{(2)} [E_x + E_y]^2$$

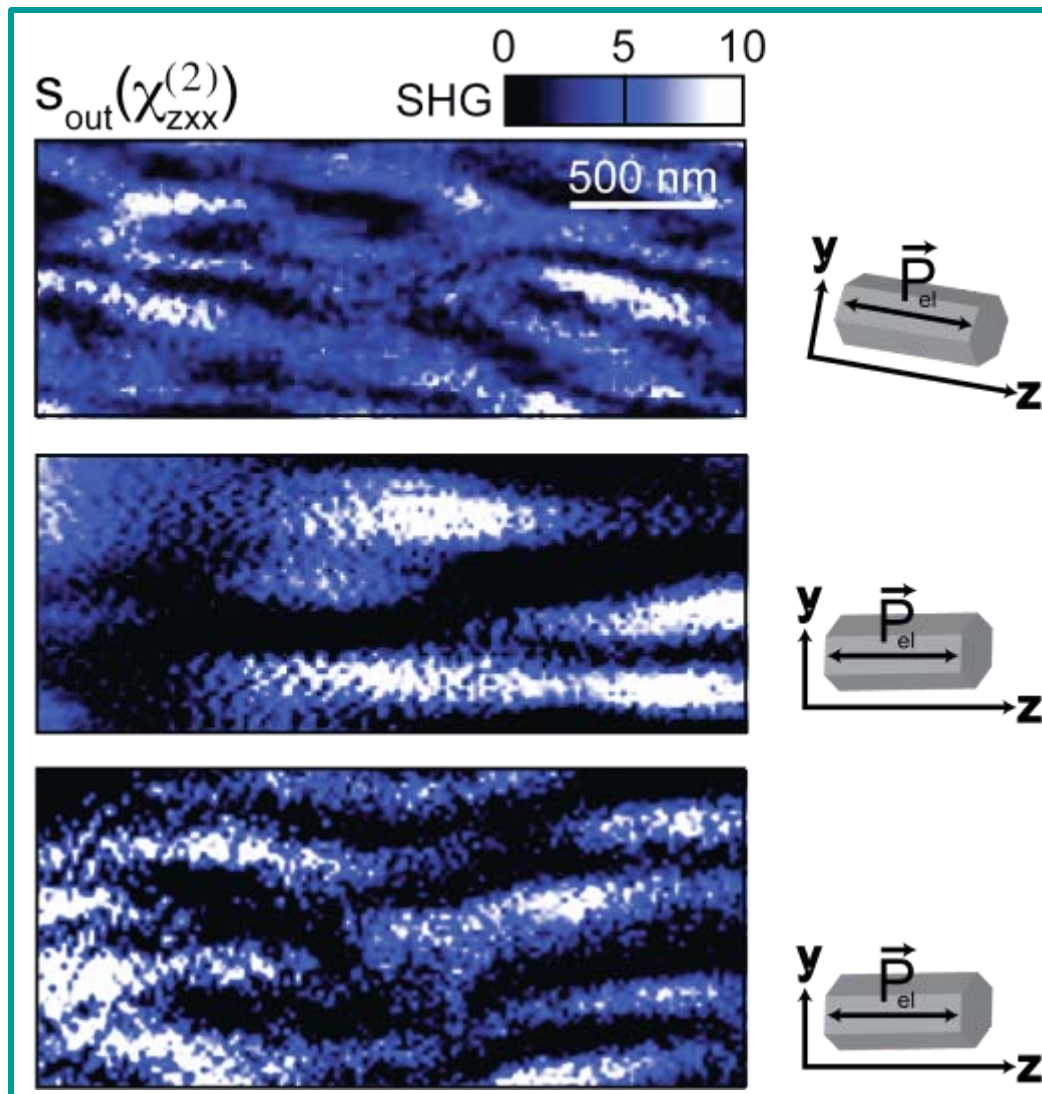
Tip-sample distance dependence



Far-field self-homodyne reference

Near-field enhanced contribution

Imaging of FEL Domains in YMnO_3



Domain dimensions:
> 100 nm wide (y)
~ 1 μm long (z)

Ferroelectric domains

Extended along
the hexagonal axis z



Parallel with \mathbf{p}_z

Part III - Experimental Techniques

Surfaces & interfaces

First Magnetic SHG Experiment

VOLUME 67, NUMBER 20

PHYSICAL REVIEW LETTERS

11 NOVEMBER 1991

Effects of Surface Magnetism on Optical Second Harmonic Generation

J. Reif, J. C. Zink, C.-M. Schneider, and J. Kirschner

Institut für Experimentalphysik, Freie Universität Berlin, Arnimallee 14, W-1000 Berlin 33, Germany

(Received 21 May 1991)

We report on the first experiments showing the influence of surface magnetization on optical second harmonic generation in reflection at a Fe(110) surface. The magneto-optical Kerr effect modifies the hyperpolarizability of the surface in the optical field, leading to a dependence of the second harmonic yield on the direction of magnetization relative to the light fields. For the clean surface an effect of 25% was determined, which decays exponentially with surface contamination by the residual gas, thus demonstrating the high surface sensitivity of this technique.

PACS numbers: 75.30.Pd, 78.20.Ls, 78.65.Ez

2878

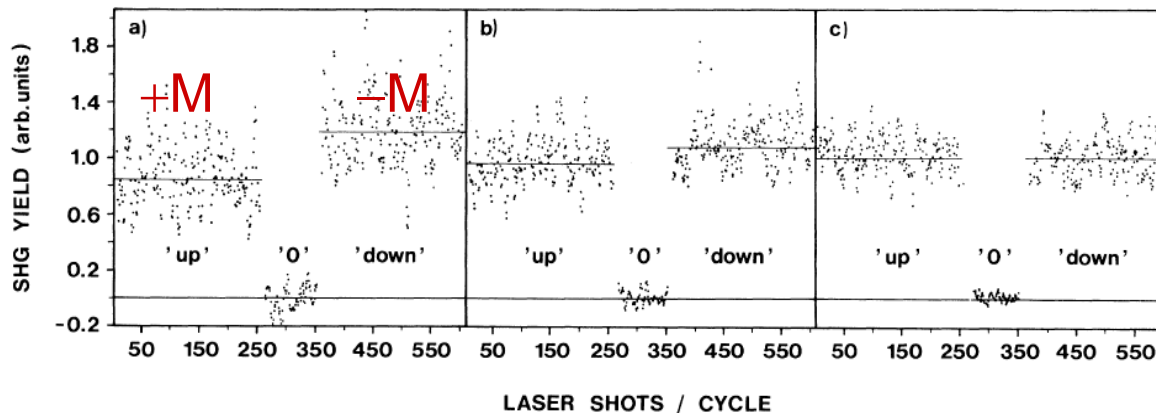
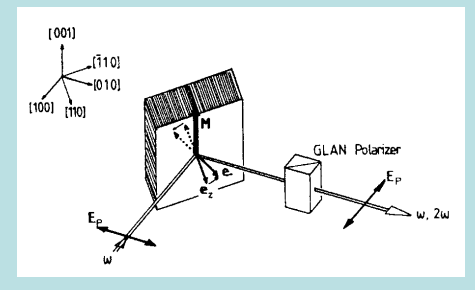


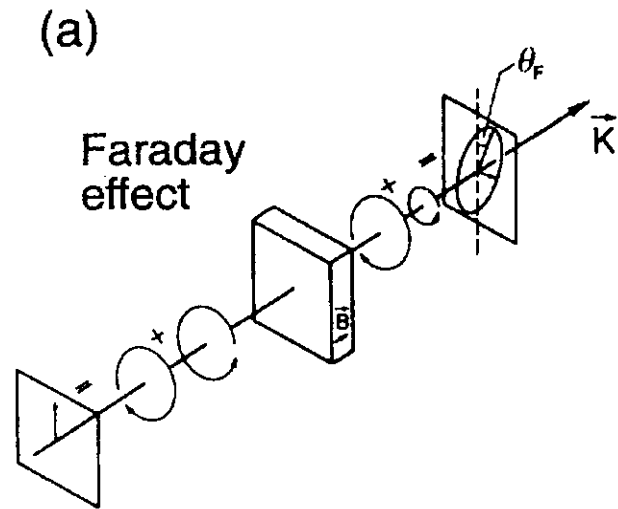
FIG. 2. Relative magnetization dependence of second harmonic signal for three different times elapsed since sample preparation [(a) ≈ 45 min, (b) ≈ 60 min, (c) ≥ 180 min]. Shown is, in each panel, an averaged [superposition of (a) 220, (b) 550, and (c) 750 cycles] experimental cycle, consisting of 250 pulses with magnetization "up," 100 pulses with no SHG signal (obtained by means of a UV blocking glass filter), and 250 pulses with magnetization "down." All signals are normalized to the expected value without influence of magnetization [cf. Eq. (1)]. The solid lines represent the average of the respective regions of interest.

Observation of a second harmonic contribution which depends on the magnetization of a Fe(001) surface

Small signal, but with high contrast \rightarrow typical for SHG!



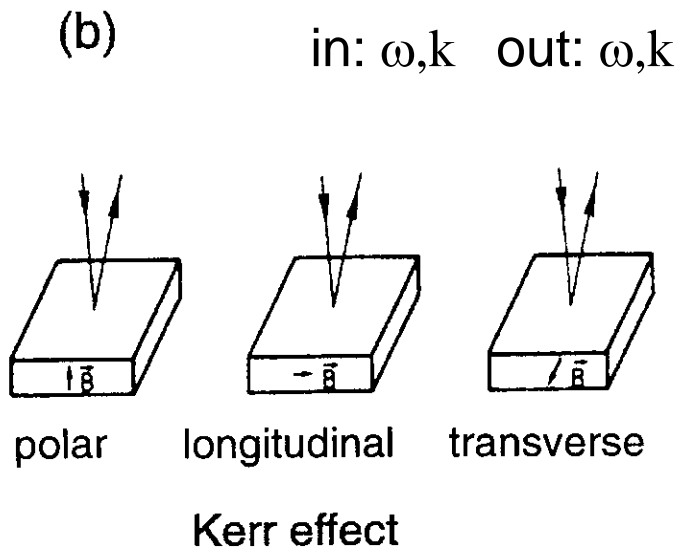
Linear Magneto-Optical Effects



Dielectric function :

$$\tilde{\epsilon} = \epsilon \begin{pmatrix} 1 & iQ & 0 \\ -iQ & 1 & 0 \\ 0 & 0 & 1 \end{pmatrix}$$

- Rotation of plane of polarization upon transmission/reflection on magnetized medium
- Described by non-diagonal elements of 3×3 matrix
- $Q \ll 1 \Rightarrow$ **small effect** ($10^{-2} \dots 10^{-5}$)



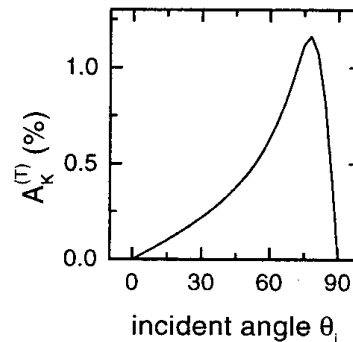
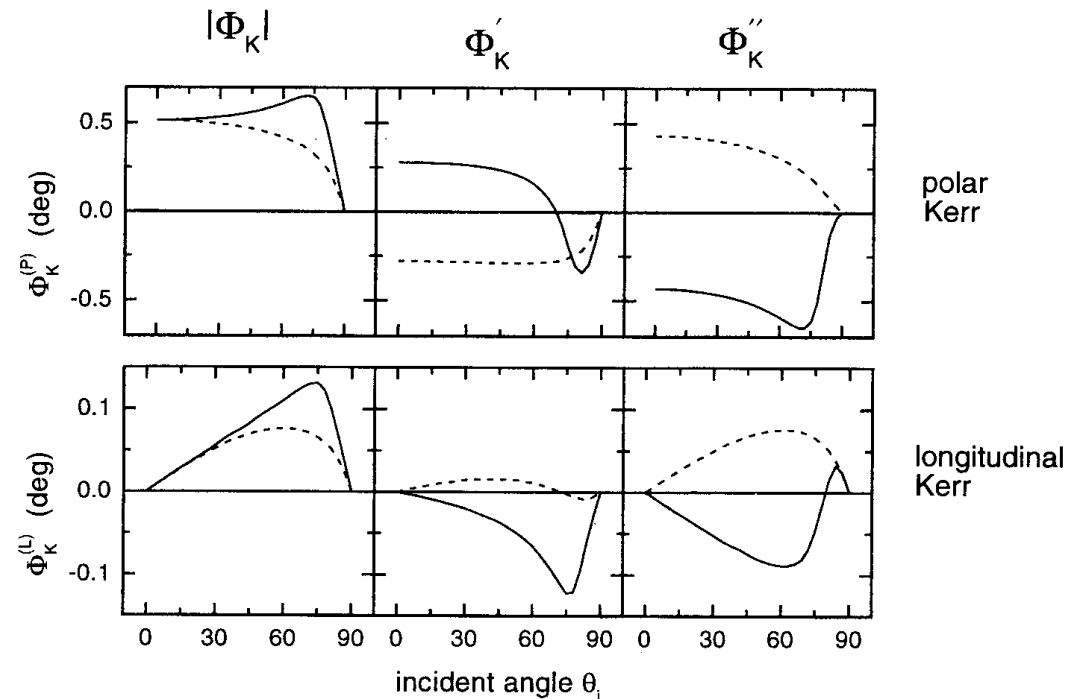
R. Vollmer in "Nonlinear Optics in Metals", Clarendon (1998)

Linear Magneto-Optical Effects

Kerr rotation
and ellipticity

$$\Phi_{Ks} = \Phi'_{Ks} + i\Phi''_{Ks} = \frac{E_p^{(r)}}{E_s^{(r)}}$$

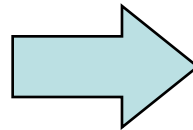
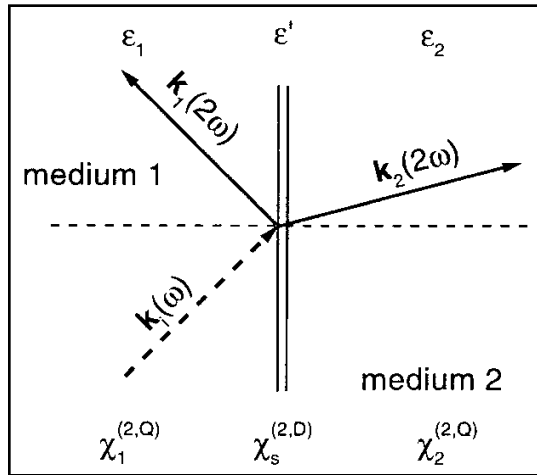
$$\Phi_{Kp} = \Phi'_{Kp} + i\Phi''_{Kp} = \frac{E_s^{(r)}}{E_p^{(r)}}$$



Fe at 800 nm
(calculated)

transverse
Kerr

Nonlinear Magneto-Optical Effects



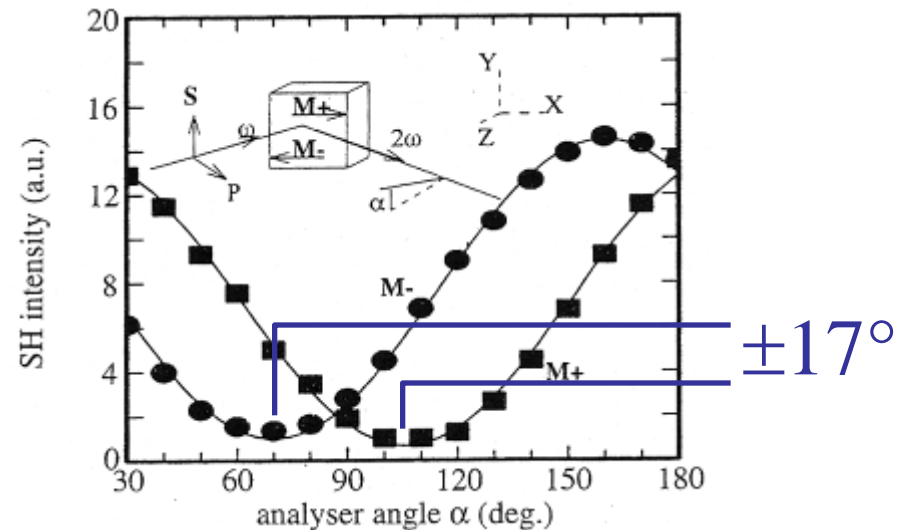
Generation of reflected SH wave:

$$P_i(2\omega) = \chi^{(2)}_{ijk}(M) E_j(\omega) E_k(\omega)$$

with $\chi^{(2)}(-M) = -\chi^{(2)}(+M)$

$\Rightarrow \chi^{(2)}$ is 3rd-rank c-tensor

NOMOKE:
NOnlinear **M**agneto-**O**ptical
Kerr-**E**ffect
 High effects of several tenth
 of degrees!



B. Koopmans et al. Phys.
 Rev. Lett. 74, 3692 (1995)

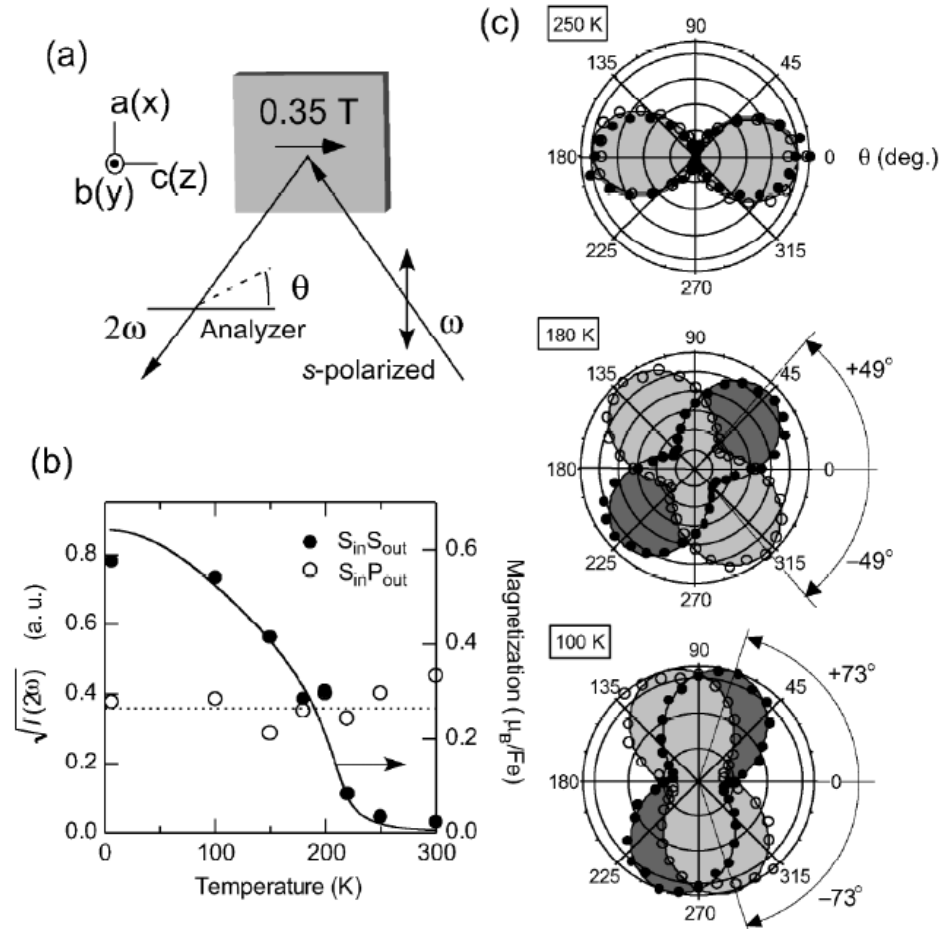
NOMOKE on a Polar Ferromagnet

GaFeO₃:

- Pyroelectric
- Ferromagnetic $T_C = 205$ K

Crystallographic
+ magnetic SHG:

$$\vec{P}(2\omega) = \epsilon_0 \begin{pmatrix} \chi_{xxx}^m \\ \chi_{yxx}^{cry} + \chi_{yxx}^m \\ 0 \end{pmatrix} E_x^2(\omega).$$

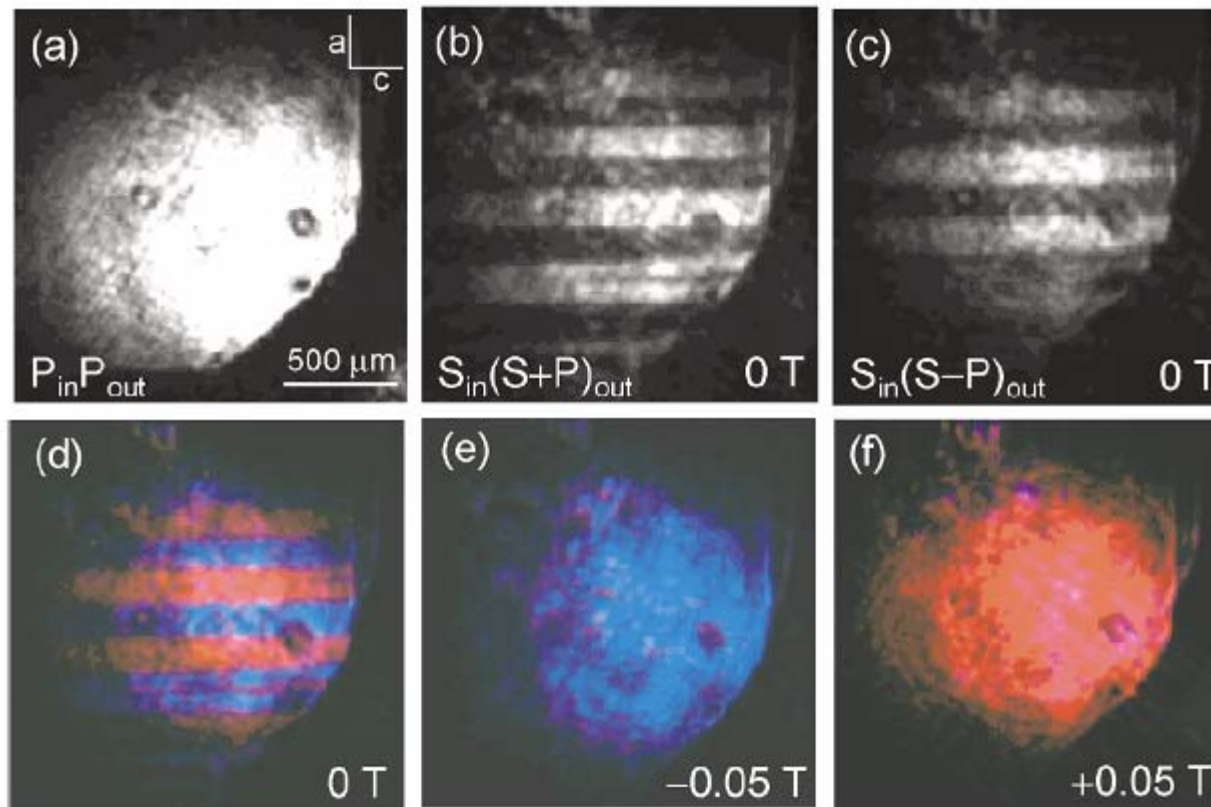


Ogawa, et.al., Phys. Rev. Lett. 92, 047401 (2004)

Magnetic Domain Imaging

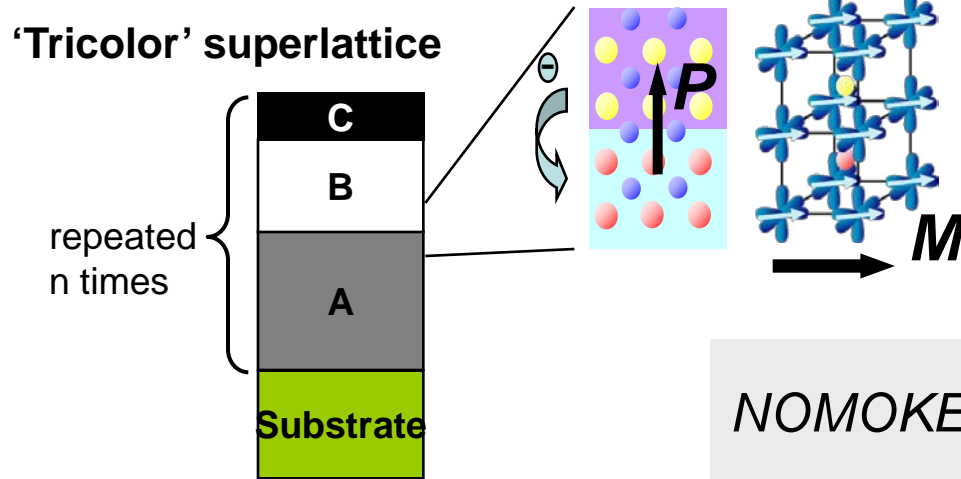
Crystalsurface

Magnetic domains



Ogawa, et.al., Phys. Rev. Lett. 92, 047401 (2004)

Interface Sensitivity



Transition metal oxide superlattices:

Charge transfer \Rightarrow **polarization**

orbital ordering \Rightarrow **magnetization**

Time & spatial inversion symmetry only broken at AB-interface \Rightarrow **SHG**

Polarization SHG $\propto P$

$$P_p^{nm}(2\omega) \propto \chi^{nm} E_s(\omega) E_s(\omega)$$

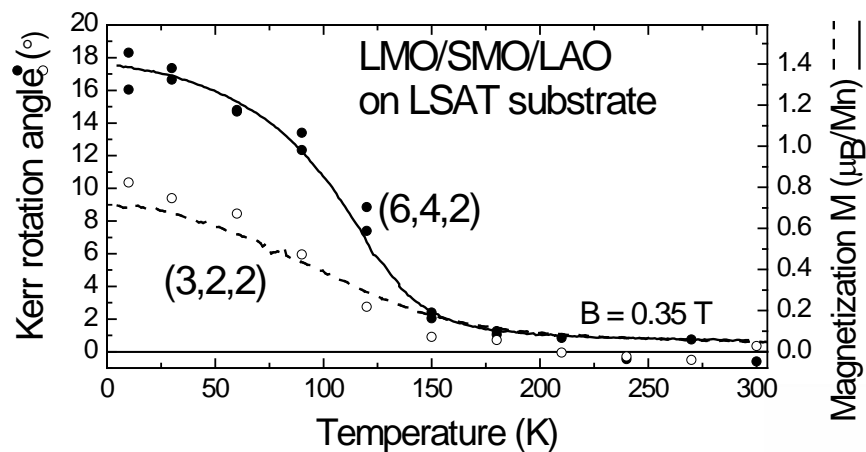
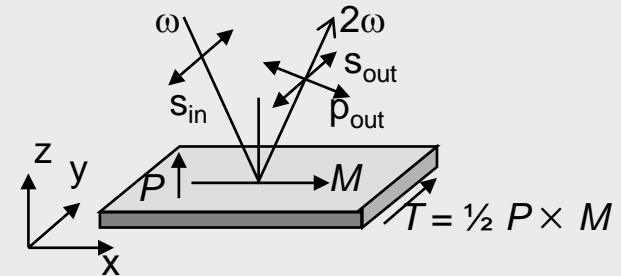
Magnetic SHG $\propto T = P \times M$

$$P_s^m(2\omega) \propto \chi^m E_s(\omega) E_s(\omega)$$

$$\chi^m := \chi^m(B)$$

NOMOKE:

$$\tan \phi = \frac{P_s^m}{P_p^{nm} \tan \Theta}$$

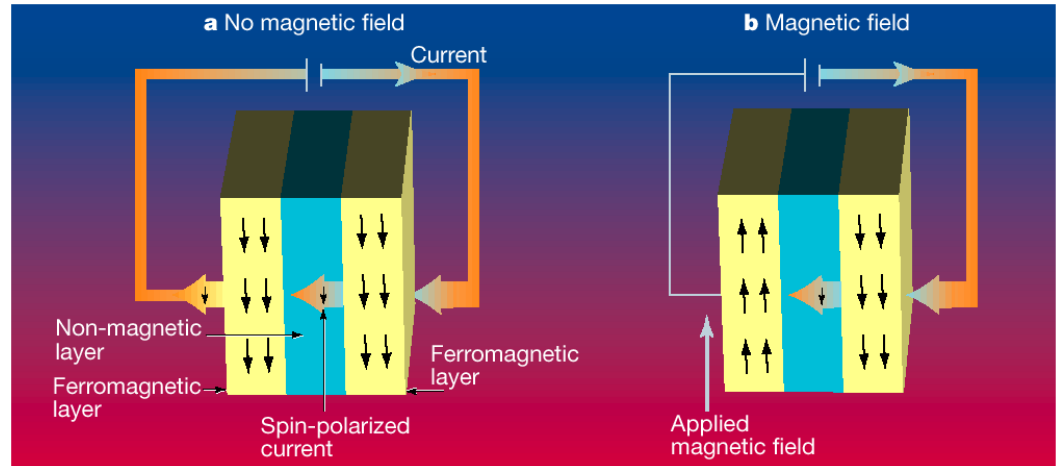


Part III - Experimental Techniques

Ultrafast nonlinear optics

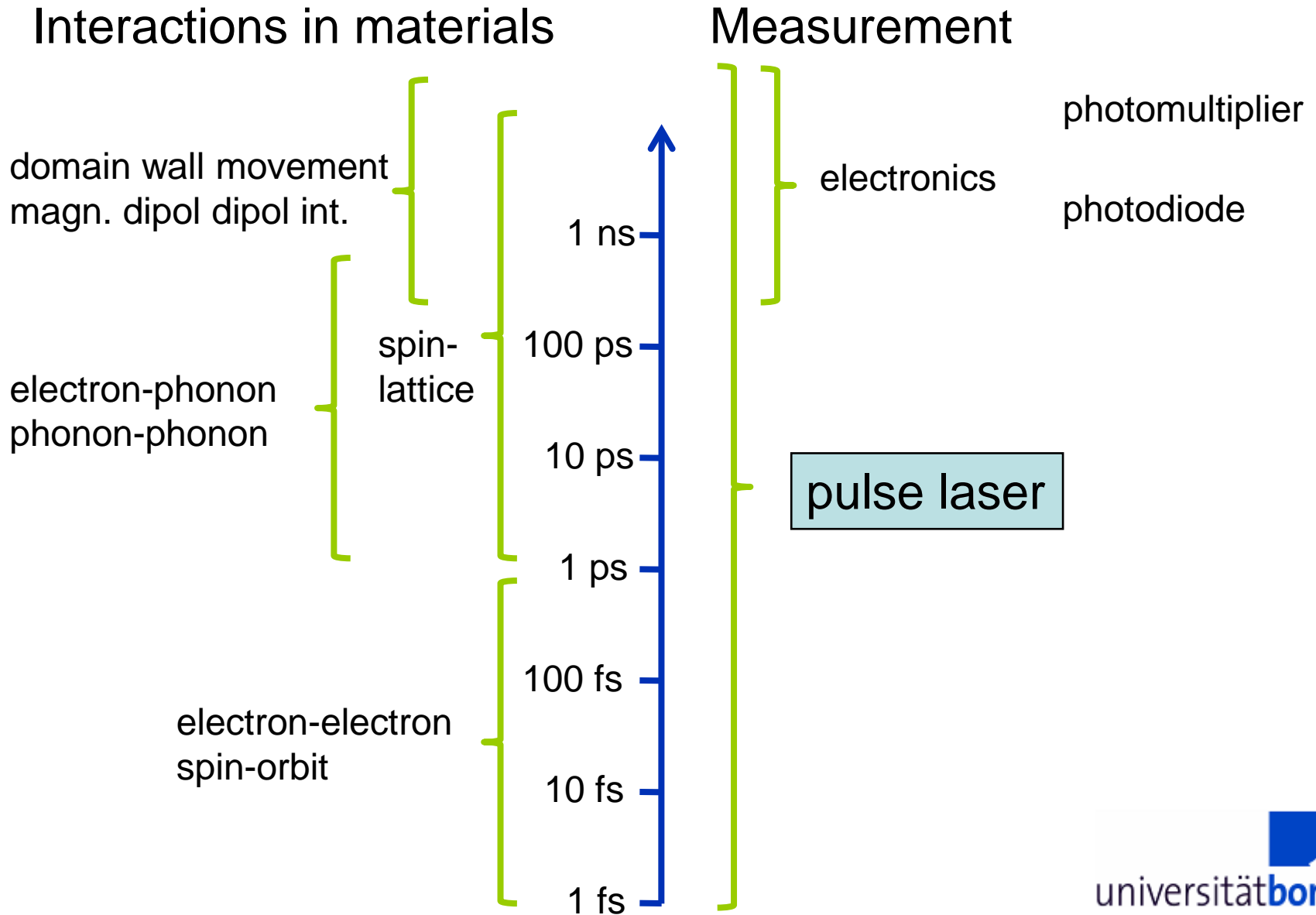
Technological Needs

- data storage
- data transfer
- etc.



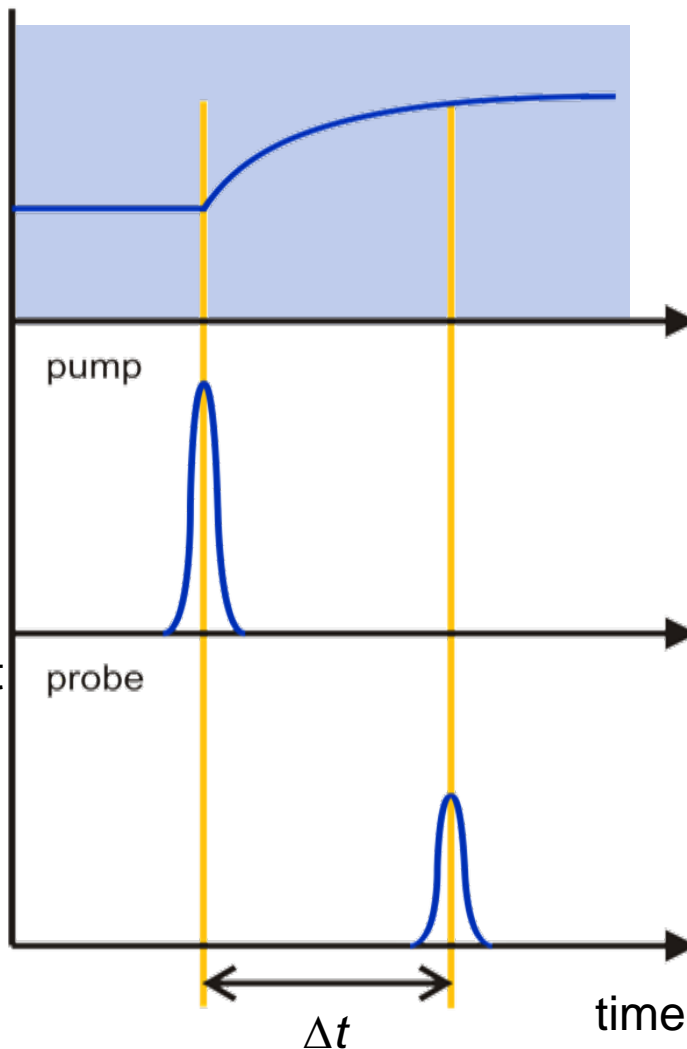
Where are the physical limits?

Timescales

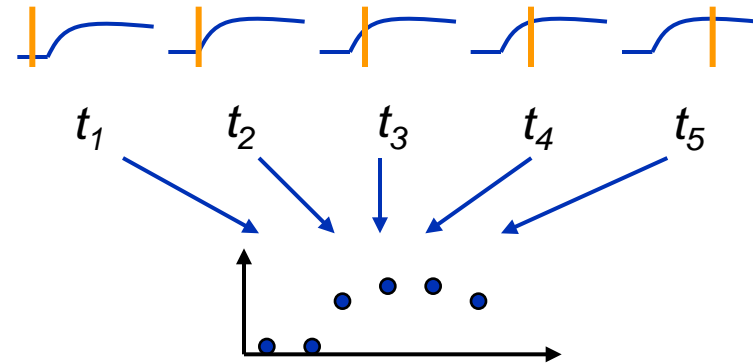


Time Resolved Pump-Probe Experiments

pump-probe scheme



stroboscopic method



excitation

Excitation

- optic
- magnetic
- etc.

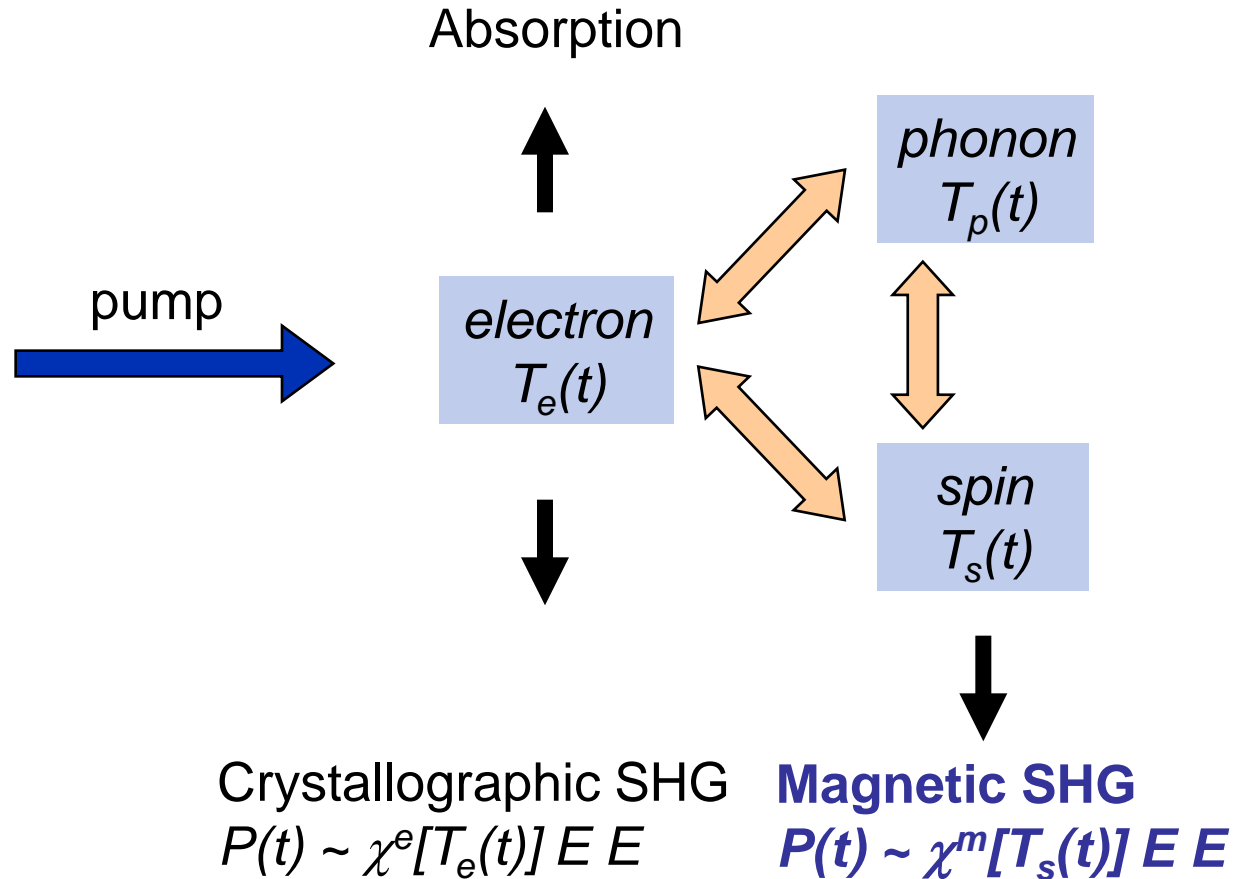
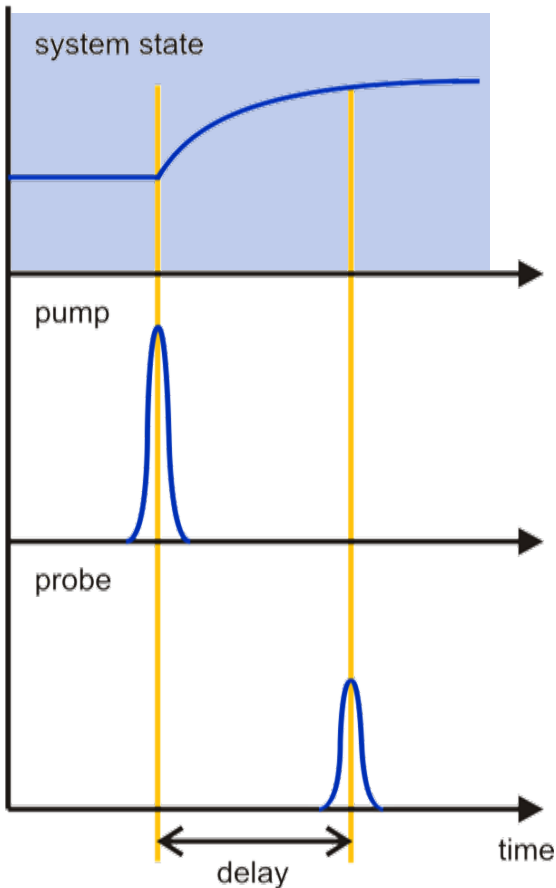
measurement

Measurement

linear/**nonlinear** optical effects

Three-Temperature Modell

pump-probe scheme



fs-Laser System

